From ethyl biodiesel to biolubricants: Options for an Indian mustard integrated biorefinery toward a green and circular economy

Jing Chen, Xiaoqiang Bian, Graeme Rapp, James Lang, Alejandro Montoya, Richard Trethowan, Brice Bouyssière, Jean-François Portha, Jean-Noël Jaubert, Peter Pratt, et al.

From Ethyl Biodiesel to Biolubricants: Options for an Indian Mustard Integrated Biorefinery towards a Green and Circular Economy

Jing Chen [a], *Xiaoqiang Bian* [a], *Graeme Rapp* [b], *James Lang* [c], *Alejandro Montoya* [c], *Richard Trethowan* [b], *Brice Bouyssiere* [d], *Jean-François Portha* [a], *Jean-Noël Jaubert* [a], *Peter Pratt* [e], *and Lucie Coniglio* [a *]

[a] Université de Lorraine - Ecole Nationale Supérieure des Industries Chimiques de Nancy, Laboratoire Réactions et Génie des Procédés UMR CNRS 7274, 1, rue Grandville BP 20451, 54001 Nancy Cedex, France; jng.chen@univ-lorraine.fr (Jing Chen); xiaoqiang.bian@univ-lorraine.fr (Xiaoqiang Bian); jean-francois.portha@univ-lorraine.fr (Jean-François Portha); jean-noel.jaubert@univ-lorraine.fr (Jean-Noël Jaubert); lucie.coniglio@univ-lorraine.fr (Lucie Coniglio)

[b] The University of Sydney, Plant Breeding Institute, I.A. Watson International Grains Research Centre, PO Box 219, Narrabri, NSW 2390, Australia; graeme.rapp@sydney.edu.au (Graeme Rapp); richard.trethowan@sydney.edu.au (Richard Trethowan)

[c] School of Chemical and Biomolecular Engineering, The University of Sydney, NSW 2006, Australia; james.lang@sydney.edu.au (James Lang); alejandro.montoya@sydney.edu.au (Alejandro Montoya)

[d] CNRS / UNIV Pau & Pays de l'Adour, Institut des Sciences Analytiques et de Physico-Chimie pour l'Environnement et les Matériaux, UMR 5254, 64000 Pau, France; brice.bouyssiere@univ-pau.fr (Brice Bouyssiere)

[e] Ineos Enterprises France, Z.I. Baleycourt BP 10095, 55103 Verdun, France; peter.pratt@ineos.com (Peter Pratt)

* To whom correspondence should be addressed. E-mail: lucie.coniglio@univ-lorraine.fr

Abstract

This work aims to analyze whether Indian mustard can be harnessed within a biorefinery system to generate energy carriers and high value-added products. Within this objective, two options of harnessing Indian mustard seed oil (IMSO) were investigated, the first for the production of ethyl biodiesel (IMSOEEs) and the second for the production of a biolubricant (IMSO2E1HEs) by transesterification of the unpurified IMSOEEs with 2-ethyl-1-hexanol (2E1H). Furthermore, low cost and environmentally-friendly conversion processes were targeted. The biofuel was obtained under mild conditions of ethanolysis (35°C, atmospheric pressure, ethanol to oil molar ratio of 8, 1.1 wt % KOH, and 50 min) carried out in two-stages separated by addition of recycled glycerol, and followed by dry-purification with Indian mustard stems-based adsorbent. In order to enhance biolubricant yield, reactive distillation with optimized operating pressure was selected (0.05 bar, 70°C, 2 wt % KOH, 2E1H to IMSOEEs molar ratio of 2, 65 min), followed by bubble-washing (assisted with citric acid) and then vacuum distillation (inferior to 0.01 bar). The produced IMSOEEs met the basic biodiesel properties with a satisfactory ester content (95.8 wt %). Similarly, a high conversion of IMOEEs (93 wt %) was reached for the biolubricant, leading to an IMSO2E1HE product that exhibited satisfactory properties, and thus has the potential to act as a biolubricant. Nevertheless, these results could be improved with a pre-treatment of the departure IMSO to remove species that are not glycerides, such as glucosinolates. Thereby, ensuring that the produced ethyl biodiesel conforms strictly to industry specifications.

Keywords: ethyl biodiesel; biolubricant; Indian mustard; biorefinery concept; low cost production

Abbreviations

ALSI	Automatic liquid sampler injector system
AES	Atomic Emission Spectrometry
BET	Brunauer-Emmet-Teller
DGs	Diacylglycerides (or diglycerides)
EC	Ethyl cellulose
EDS	Energy dispersive X-ray spectroscopy
Ethyl C18:1	Ethyl oleate
Ethyl C18:2	Ethyl linoleate
Ethyl C18:3	Ethyl linolenate
2E1H C18:1	2-Ethyl-1-hexyl oleate
2E1H C18:2	2-Ethyl-1-hexyl linoleate
2E1H C18:1	2-Ethyl-1-hexyl linolenate
FAEEs	Fatty acid ethyl esters
FAMEs	Fatty acid methyl esters
FFAs	Free fatty acids
FID	Flame ionization detector
FIMS	Fine Indian mustard stems
GC	Gas-chromatography
IMSO	Indian mustard seed oil
IMSOy	Indian mustard seed oil obtained from yellow seeds
IMSOb	Indian mustard seed oil obtained from brown seeds
IMSOEEs	Indian mustard seed oil ethyl esters (ethyl biodiesel)
IMSOyEEs	Ethyl esters of Indian mustard seed oil (ethyl biodiesel) obtained from yellow seeds
IMSObEEs	Ethyl esters of Indian mustard seed oil (ethyl biodiesel) obtained from brown seeds
IMSO2E1HE	Indian mustard seed oil 2-ethyl-1-hexyl ester (biolubricant)
IS	Internal standard
[KOH]	Potassium hydroxide concentration
MGs	Monoacylglycerides (or monoglycerides)
MHD	Methyl heptadecanoate
MR	Molar ratio
MS	Mass spectrometry

NEVO	Non-edible vegetable oil
S.I.	Supporting information
SEM	Scanning electron microscopy
STP	Standard temperature and pressure (T = 273.15 K; P = 10^5 Pa)
TGs	Triacylglycerides (or triglycerides)
2E1H	2-ethyl-1-hexanol

1. Introduction

Biomass harnessed within the biorefinery concept that involves low cost and environmentally-friendly conversion processes to generate energy carriers and high value-added products is essential for a sustainable plant-based industry (**Coniglio et al., 2014; Navarro-Pineda et al., 2016; Raman et al., 2018**). Mustard is an important commercial plant across the world that is used for food and oil production and can naturally be integrated within a synergetic cropping system.

Indian mustard is a hardy, drought and disease resistant species with biofumigation properties that provides a chemical-free disease suppression in subsequent cereal crops, such as wheat and barley (**Kirkegaard and Sarwar, 1999; Handiseni et al., 2012; Ngala et al., 2015**). Cultivation of Indian mustard as a rotational crop for oil production is more versatile than other perennial plants, such as *Pongamia* trees, because the annual growth cycle is faster, reducing establishment costs, time to product delivery, and therefore, is ideal in climate change conditions (**Boomiraj et al., 2010; Singh et al., 2018**). The Indian mustard oil production and processing leave many valuable components which have potential to improve the commercial viability in an integrated biorefinery. For instance, pharmaceutical, veterinary, agricultural and animal food products can be obtained from the meal due to the high content of glucosinolates, proteins and fibre, and bioethanol and biogas can be obtained from the digestion of residues for energy generation. Mustard oils naturally contain a high erucic acid content which is harmful to human health (**Tabtabaei et al., 2014**). This has been reduced by selective breeding, enabling it to compete with canola as cooking vegetable oil (**Rapp, 2018**). Nevertheless in the context of a rotation crop for biofumigation, biodiesel and biolubricants can be obtained from the seed oil with limited environmental footprint, and it has been shown that high erucic acid varieties provide biodiesel with superior lubricating properties (**Tabtabaei et al., 2014**).

With reference to the production of biolubricants and biodiesel, vegetable oils (or any lipid sources) require first chemical modifications to obtain the esters that meet the desired properties and fulfill the standards in terms of performance. Regarding biolubricants (or bio-based lubricants), the three main chemical routes currently used to enhance vegetable oil properties targeted for this application, i.e. cold flow properties and thermal-oxidative stability, are: *(i)* esterification or transesterification, *(ii)* estolide formation, and *(iii)* epoxidation followed by ring opening and acetylation (**McNutt et al., 2016; Syahir et al., 2017; Chan et al., 2018**). The first route requires high oleic base stocks to produce biolubricants meeting requirements and high vacuum conditions to decrease the reaction temperature. The second route requires a lower reaction temperature but often needs capping fatty acids which are expensive reactants (**Cermak et al., 2013; Syahir et al., 2017**). Hence, to reduce the production cost by extending the potential sales markets, **de Haro et al. (2018)** developed a three-step process leading to methyl biodiesel and choline carboxylates (biosurfactants), in addition to estolide methyl esters (biolubricant). The third route requires multiple reaction stages making it economically unfavorable, although the final product exhibits ideal lubricant properties (**McNutt et al., 2016**). Moreover, vegetable oil modifications by estolide formation or epoxidation followed by ring opening and acetylation mainly occur under homogeneous acid catalysis, which involves catalyst loss and potential corrosion issues during process operation. By contrast, the transesterification of vegetable oils with long-chain alcohols (containing more than 5 carbon atoms) or polyols (trimethylolpropane) may be carried out under homogeneous or heterogeneous basic catalysis, with additionally a shorter reaction time compared with acid catalysis (**Zheng et al., 2018**); the latest tendency being the enzymatic catalysis (**Cerón et al., 2018**) extended to the esterification (**Kim et al. 2019**) to operate under mild conditions, but at the cost of a longer reaction time. Regarding biodiesel production, transesterification with a short-chain alcohol (methanol or ethanol) is the most widely used route to convert vegetable oils into biodiesel, exhibiting much better engine performance and emission characteristics; not to mention a much lower viscosity to avoid engine failure (**Coniglio et al., 2013**).

This work investigates two aspects of harnessing Indian mustard seed oil (IMSO), the first for production of ethyl biodiesel (energy carrier) and the second for conversion of the produced ethyl biodiesel into biolubricant (high-added value product). Both ethyl biodiesel and biolubricant are produced via a common conversion process (KOH-based transesterification). This flexibility is particularly suitable as crude oil prices fluctuate and the global demand for lubricants is expected to increase by 2.0% per year to 45.40 million metric tons in 2020, with the share of bio-based lubricant market projected to rise to 15-30%. This shift towards

biolubricants is mainly due to their high biodegradability, low aquatic toxicity, and renewability, as they are mainly derived from vegetable oils (**Karmakar et al., 2017; Panchal et al., 2017; Hossain et al., 2018**). Hence, thanks to their polar attraction to metals induced by the chemical structure of their base stocks, biolubricants often perform better than conventional mineral oil-based lubricants. Indeed, biolubricants exhibit higher adhesiveness, lubricity, and thereby reduced frictional losses in engines and machinery, lowering energy or fuel consumption, and subsequently decreasing harmful gases emissions (**Syahir et al., 2017; Chan et al., 2018; Hossain et al., 2018**). The development of economic and green processes for the production of biolubricants to replace mineral oil-based lubricants is thus critical (**Karmakar et al., 2017**), especially from cheaper and reliable feedstocks (**Wang et al., 2014; Syahir et al., 2017**).

While ethanol was selected to conduct the transesterification reaction leading to the targeted biofuel, the alcohol commonly used to obtain the targeted biolubricant for metalworking applications is 2-ethyl-1-hexanol (**Habib et al., 2014; Kleinaitė et al., 2014; Trivedi et al., 2015; Geethanjali et al., 2016; Syahir et al., 2017; Zheng et al., 2018**). Ethyl biodiesel (fatty acid ethyl esters, FAEEs) was preferred to the commonly commercialized methyl biodiesel (fatty acid methyl esters, FAMEs) for two main reasons: *(i)* apart from being non-toxic, bioethanol may be produced from agricultural resources and residues, leading thus to a 100% renewable biodiesel (**Brunschwig et al., 2012; Coniglio et al., 2014; Navarro-Pineda et al., 2016**); *(ii)* FAEEs have better biodegradability, higher flash point, improved cold-flow properties and oxidation stability, and lower emissions of NOx, CO, and ultrafine particles than FAMEs (**Coniglio et al., 2013**). Furthermore, fusel oil obtained as by-product of ethanol fermentation and composed mainly of isoamyl alcohol has been used successfully to produce biolubricant by transesterification of palm kernel oil (**Cerón et al., 2018**). Hence, a major part of ethanol production industry could be integrated in the proposed process to yield biodiesel (by using ethanol) and biolubricant (by using fusel oil), limiting material inputs, production costs, and environmental impacts.

Apart from the development of a conversion process focused on a sustainable plant-based industry, the novelty of this work is at two levels. Firstly, while the production of biodiesel using the selected method (KOH-based ethanolysis with addition of recycled glycerol followed by dry-purification with a natural adsorbent, the whole conducted under "ambient" conditions) has proven to be efficient, low-cost, and environmentally-friendly for various non-edible vegetable oils (NEVOs) (**Nitièma-Yefanova et al., 2017**), it has never been validated with Indian mustard (*Brassica juncea*) by using the oil as a triglyceride source and the stems as

adsorbent. Ethanolysis of mustard (*Brassica nigra*) seed oil followed by dry-purification with activated carbon from de-oiled cake was recently performed in the literature (**Fadhil et al., 2014**), but under higher temperature. Secondly, regarding biolubricant production, the combined effect of reactive distillation and reaction pressure (mainly investigated for biolubricant synthesis by fatty acid esterification with polyols (**Maurad et al., 2018; Kim et al., 2019**)) is revealed for the first time in this work (i.e. within the framework of ethyl biodiesel transesterification with a long-chain branched alcohol such as 2-ethyl-1-hexanol).

2. Materials & Methods

A schematic representation of the catalyzed transesterification reactions that were carried out in this work for the production of ethyl biodiesel and biolubricant are described in **Figures 1-2**.

Figures 1-2

2.1. Materials

Reagents (citric acid, ethanol, glycerol, and potassium hydroxide), solvent (n-heptane) and the chromatographic standards (methyl heptadecanoate, ethyl oleate) of analytical grade were obtained from Merck, Acros Organics or Sigma-Aldrich. On the other hand, 2-ethyl-1-hexanol (> 99 %) was provided by Ineos Enterprises France. For the lipid feedstock, yellow and brown color Indian mustard seeds were used to obtain IMSOy and IMSOb samples respectively, by mechanical crushing followed by filtration (**Rapp, 2018**). Characterization of the oils in terms of fatty acid profiles and key properties with respect to ethanolysis, together with the analytical techniques used, are summarized in **Tables 1 and 2**. The natural adsorbent used in the dry-purification stage of ethyl biodiesel was prepared from Indian mustard stems, previously sundried for 2-3 days, crushed and then sieved to a particle size of 100 to 710 µm. Characterization of the obtained particles, designated FIMS, is detailed in Appendix B (**Mazivila et al., 2015; Feng et al., 2018; Rapp et al., 2018**).

Tables 1-2

2.2. From Indian mustard seed oils to ethyl biodiesel

All experiments and analyses were conducted at least in duplicate (in triplicate when disagreement was found). From each set of duplicates an average value was then calculated and provided as result (for triplicates or more, results are given is terms of average ± standard deviation).

2.2.1. Conversion of the Indian mustard seed oils

The FFA and water contents of the departure lipid feedstocks (**Table 2**) confirm that the alkali catalysis is a suitable route to produce the Indian mustard seed oil ethyl esters (IMSOEEs). Similar to **Nitièma-Yefanova et al. (2016-2017)**, a two-stage procedure with intermediate addition of glycerol to enhance ethanolysis yields was adopted. However, the various operating conditions were optimized for each lipid feedstock. The operating conditions selected in this work (together with the corresponding IMSOEE content and ethanolysis-separation yield) are summarized in **Table 3.** The catalyst and stirring parameters (speed and duration) were set once and for all (respectively to KOH and 250 rpm during the first reaction stage as this choice had showed to be the most appropriate for ethanolysis conducted in a laboratory scale setup (**Nitièma-Yefanova et al., 2016**)). By contrast, the other key variables of the ethanolysis reaction, i.e. temperature, ethanol to oil molar ratio (MR), catalyst mass concentration, mass fraction of glycerol added, were changed successively within ranges to allow an optimum set of values to be reached while satisfying our constraints (biodiesel production with low cost and high yields). In the same context, the possibility of reusing crude glycerol by-produced from previous biodiesel production runs was also assessed.

Table 3

All ethanolysis reactions were carried out in a 250 mL three-neck round bottom flask equipped with a thermometer (± 0.5°C), a reflux condenser, a sampling outlet, and a temperature-controlled magnetic stirrer system (± 1°C) with a PTFE magnetic stir bar. After weighing the desired amount of IMSO (60 g) in the dried reaction flask, the system was heated to the set temperature under constant stirring. Simultaneously, the amounts of ethanol and KOH defined for the experiment were mixed in another flask, preheated at the temperature of the experiment, and then added to the IMSO. This addition is taken as time zero of the reaction. After 30 min of reaction (end of the first stage), glycerol was added into the ethanolysis product, showing as a single pseudo-homogenous phase (start of the second stage). Following 5 min of

vigorous stirring, the ethanolysis product was then allowed to stand at ambient temperature until the end of the reaction time and subsequent phase separation. For experiments carried out under ethanol normal boiling point, the reaction mixture was cooled to ambient temperature prior to the addition of glycerol to reduce glycerol miscibility in the ester-rich phase. The reaction time was set to a sufficient value for reaching the maximum conversion (60 min). Off-line monitoring of ethanolysis was conducted by gas-chromatography coupled with a flame ionization detector (GC-FID), at a given sampling frequency (2-min intervals up to 10 min of reaction, and then 5-min intervals until the end of the experiment). The IMSOEEs were preliminary identified by GC-mass spectrometry (MS). Information specific to the GC-equipment and analysis of samples with preliminary neutralization are given in **Table A1** (Appendix A) (**EN-14103, 2011; Nitièma-Yefanova et al., 2016; Muhammad et al., 2017**).

After the reaction, the ethanolysis product was transferred into a separating funnel. The lower phase containing the introduced and liberated glycerol with entrained IMSOEEs was withdrawn first, followed by the upper-phase consisting mainly of IMSOEEs with residual glycerides and some glycerol. The ethanol remaining in each phase was then evaporated (70°C, 180 mbar, for 1.5 h) to further separate glycerol from the IMSOEEs (**Zhou and Boocock, 2006; Nitièma-Yefanova et al., 2017**). The recovered fractions of IMSOEEs were then gathered to determine the yield of the ethanolysis and separation steps according to:

$$\text{Yield (wt \%)} = \frac{\text{mass of crude IMSOEEs recovered}}{\text{initial mass of IMSO}} \times 100 \quad (1)$$

The IMSOEE samples of runs with high ester contents and yields were collected to obtain a single pool from which a fraction was further purified by dry-washing (section 2.2.2); the remainder was dedicated to biolubricant production (section 2.3).

2.2.2. Purification of IMSOEEs and fuel property evaluation

The IMSOEEs were mixed with a specified amount of the natural adsorbent to remove residual catalyst, glycerol and other impurities. The procedure was modified from previous work (**Nitièma-Yefanova et al., 2015; 2017**). A three stage dry-washing was conducted with, for each treatment cycle, 4 wt % of adsorbent in the unpurified IMSOEE sample maintained under stirring for 20 min at 35°C, followed by vacuum filtration. Details of the equipment and operating conditions used to characterize the IMSOEEs before and after dry-washing on the FIMS adsorbent are summarized in **Table A1** (Appendix A) (**EN-ISO-12937, 2000; Pohl et**

al., 2010; Caumette et al., 2010; EN-14105, 2011; EN-14103, 2011; Nitièma-Yefanova et al., 2015; Muhammad et al., 2017). Characterization was achieved by considering molecular species such as triacylglycerides (TGs), diacylglycerides (DGs), monoacylglycerides (MGs), free glycerin, water and IMSOEEs, and also potassium and heavy metals (brought into the IMSOEEs via the catalyst used and the IMSO extraction stage). Some fuel properties of the resulting ethyl biodiesel (acid value, color, density, viscosity, flash point, cloud point, and pour point) were also evaluated in accordance to ASTM or ISO standards (**Table A1**, Appendix A) (EN-ISO-12185, 1996; EN-ISO-3104, 1996; EN-14104, 2003; ASTM D1544-04, 2010; Carareto et al., 2012; Bolonio et al., 2015).

2.3. From ethyl biodiesel to biolubricant

The fraction of IMSOEEs that was not dedicated to purification (section 2.2.2) was converted by alkaline transesterification with 2-ethyl-1-hexanol (2E1H) to obtain the targeted biolubricant, i.e. IMSO-based 2-ethyl-1-hexyl esters (IMSO2E1HEs). As KOH used in excess during ethanolysis was not removed from the IMSOEEs, the same catalyst was naturally used for this additional transesterification step. The characteristics of the IMSOEEs used here as the departure reactants (composition in molecular species including KOH content) are given in **Table 4** for the IMSOEEs before purification.

Table 4

2.3.1. Conversion of ethyl biodiesel

Biolubricant synthesis was carried out in a laboratory scale batch reactive distillation unit operating under low pressure. This option has two main positive features: *(i)* to reduce both reaction temperature and reaction time leading to minimized energy costs; *(ii)* to remove ethanol (by-product) by distillation from the reacting mixture, leading to increased biolubricant yield by shifting the transesterification chemical equilibrium in favor of product formation. The selected reactive distillation method (thus somewhat different to the commonly used method with a reflux condenser (Habib et al., 2014)) should help operating under a less severe vacuum. Therefore, the impact of operating pressure on the transesterification (which has never been investigated to the best of the authors' knowledge) was analyzed for three low pressure conditions: 0.05, 0.1, and 0.5 bar. By contrast, the other key transesterification parameters were kept constant (**Table 5a**): reaction temperature set at 70°C (Habib et al., 2014) (i.e. few degrees under the boiling point of 2E1H at 0.01 bar), 2 wt % of KOH (Habib et al., 2014) (on basis of

the initial IMSOEE mass), MR (2E1H to IMSOEEs) = 2 (i.e. twice the stoichiometric value to shift even more the reaction chemical equilibrium towards products formation), with a reaction time long enough to promote conversion of IMSOEEs (65 min).

Table 5

Similarly to IMSO ethanolysis, all transesterification reactions of ethyl biodiesel to biolubricant were conducted in a 250 mL three-neck round bottom flask equipped with a thermometer (± 0.5°C), a sampling outlet, and a temperature-controlled magnetic stirrer system (± 1°C) with a PTFE magnetic stir bar. However, the reflux condenser was replaced by a Vigreux column surmounted by a second thermometer (± 0.5°C) and connected, on the side, to a Liebig condenser. This was in turn connected to a vacuum take-off adapter for attachment via a three-way valve to the vacuum pump and to two flasks for collecting distillated ethanol. The Liebig condenser was cooled with a recirculating silicon oil bath (0°C) and the two collection flasks with an ice bath (for bulk reasons). In the procedure, crude IMSOEEs (50 g) corresponding to 44.06 g of FAEEs (content before purification: 88.1 wt %, **Table 4**; average molecular weight: 313, **Table 1**) were weighed directly in the dried reaction flask and were then heated to the selected temperature. Simultaneously, to generate the active species of the catalyst *in situ*, 2E1H (36.71 g) and KOH (0.8812 g) were mixed in another flask, preheated at the temperature of the experiment and then added to the IMSOEEs. The three-way valve was then switched for connecting the reactive distillation unit to the vacuum pump. This point was considered as time zero of the reaction which was monitored off-line by GC-FID at a given sampling frequency (10-min intervals until the end of the experiment, after a first sampling at 4 min reaction time). Similar to IMSOEEs, preliminary identification of the IMSO2E1HEs was conducted by GC-MS, and information specific to the GC-equipment and sample analysis are given in **Table A1** (Appendix A) (**EN-14103, 2011; Nitièma-Yefanova et al., 2016; Muhammad et al., 2017**).

The yield of biolubricant was estimated by:

$$\text{Yield}\ (\%) = \frac{(m_{IMSO2E1HEs})_{\text{actual}}}{(m_{IMSO2E1HEs})_{\text{theoritical}}} \times 100 \qquad (2)$$

with: $(m_{IMSO2E1HEs})_{\text{actual}} = m^{crude}_{IMSO2E1HEs} \cdot \bar{x}_{IMSO2E1HEs}$ and

$$(m_{IMSO2E1HEs})_{\text{theoritical}} = \frac{\vartheta_{IMSO2E1Hs}}{\vartheta_{IMSOEEs}} \cdot \frac{m^{crude}_{IMSOEEs} \cdot \bar{x}_{IMSOEEs}}{M_{w\,IMSOEEs}} \cdot M_{w\,IMSO2E1HEs}$$

where ϑ_i is the stoichiometric coefficient of species i of molecular weight $M_{w\,i}$ and occurring in the reacting mixture k of mass m_k^{crude} with a mass fraction $\bar{x}_i$. As illustrated in **Figure 2**, $\vartheta_{IMSOEEs}$ and $\vartheta_{IMSO2E1Hs}$ are both equal to unity.

2.3.2. Purification of IMSO2E1HEs and biolubricant property evaluation

The crude IMSO2E1HEs were purified by batch bubble-washing conducted at 35°C, 1 atm, with a 4 wt% citric acid solution in distilled water at first, and then only distilled water. Washing solution and esters (respective volume proportions: 1/3 and 2/3) were poured in a separating funnel equipped inside with a fritted glass cannula connected to an air pump via a control valve. Purification batches were carried out by replacing the contaminated washing solution until potassium concentration in the aqueous phase remained constant (analysis by Flame Atomic Emission Spectroscopy (Flame-AES), **Table A1**, Appendix A). After bubble-washing to remove catalyst (with residual ethanol and potential traces of glycerol), excess 2E1H and residual water-washing were recovered by vacuum fractional distillation (operating pressure lower than 0.01 bar with a similar equipment as the one used for the batch reactive distillation). Ester and potassium contents of the purified IMSO2E1HEs (distillation residue) were respectively determined by GG-FID (**EN-14103, 2011; Nitièma-Yefanova et al., 2016; Muhammad et al., 2017**) and ICP-AES (**Pohl et al., 2010; Caumette et al., 2010; Nitièma-Yefanova et al., 2015**), while some key biolubricant quality requirements were evaluated according to ASTM or ISO standards (**EN-ISO-12185, 1996; EN-ISO-3104, 1996; ISO-6618, 1997; ASTM D1544-04, 2010**) (**Table A1**, Appendix A).

3. Results and discussion

3.1. Ethyl biodiesel production and main performance properties

The fundamental aspects underpinning the following discussion are available in earlier published works, both for the reaction & separation stages (supporting information-Appendix A of (**Nitièma-Yefanova et al., 2016**)) and the dry-purification stage (**Nitièma-Yefanova et al., 2015**). Consequently, results will be discussed on the basis of conclusive justifications derived from these fundamental aspects.

388 *3.1.1. Reaction and separation*

389 The FAEE contents in percent mass fractions and the ethanolysis-separation yields
390 obtained for the most relevant experiments conducted in this work are presented in **Table 3**.
391 The FAEE contents as a function of time of the ethanolysis process monitored by GC-FID are
392 given in **Figures 3-6**.

393 **Figures 3-6**

394 As illustrated in **Figures 3-6**, for all operating conditions the FAEE content increases
395 rapidly during a short period, and then asymptotically approaches the first stage chemical
396 equilibrium imposed by the initial composition and temperature of the reacting mixture.
397 Furthermore, none of these FAEE profiles depict any mass transfer limitation at the early stage
398 of the reaction. Ethanol has a higher dissolving power for triglycerides than methanol.
399 Therefore, the sigmoidal profiles commonly obtained with methanolysis (under control of three
400 successive mechanisms: mass transfer, kinetics, and chemical equilibrium) are not observed
401 with ethanolysis (under control of the last two mechanisms, only). Then, after addition of
402 glycerol to initiate the second stage, the FAEE content increases sharply in the first few minutes
403 for asymptotically approaching a new chemical equilibrium state. The increment in the ester
404 content, generated during the 10 min after the glycerol addition, ranges from 3 to 9 wt %
405 depending on the initial operating conditions of the ethanolysis reaction. These increments
406 correspond to a glycerol recovery (after ethanol evaporation) of about 40 to 87 wt %, confirming
407 the two-stage procedure efficiency (glycerol performs as poorly as water for glyceride removal
408 (**Berrios et al., 2011**)).

409 Furthermore, temperature has a dual effect on IMSO ethanolysis. Indeed, when
410 ethanolysis is still under kinetic control (sharp rise of the ester profile), the temperature has a
411 positive impact, similar to catalyst concentration, by increasing the reaction rate constant
412 (Arrhenius law) thus accelerating glyceride conversion (**Figure 3**; exp. 11 vs 12 in **Figure 5**).
413 However, when ethanolysis comes under thermodynamic control (ester profile reaching a
414 plateau), temperature has a negative impact, particularly for MR approaching a critical value of
415 6:1 (plateaus of the 1st stage chemical equilibrium at 35 and 78°C far from each other in **Figure**
416 **3a**, much closer in **Figure 3b** with MR = 8:1). This behavior may firstly be explained by a
417 likely exothermicity of the IMSO ethanolysis as observed in the literature for soybean oil
418 (**Richard et al., 2013**) and some NEVOs (**Nitièma-Yefanova et al., 2017**); and secondly, by
419 the partial miscibility of glycerol into the ester-rich phase that is favored at higher temperature
420 (**Nitièma-Yefanova et al., 2016**). Nevertheless, IMSO ethanolysis should not be conducted at
421 temperatures lower than 35°C (i.e. 25°C, exp. 3 **Table 3** and **Figure 3**) although a decrease of

10°C in this temperature range does not seem to significantly impact the effect of glycerol addition (ester content increment between the 1st and 2nd stage of chemical equilibrium when reaction temperature is 35 or 25°C: 5 wt %; exp. 2 vs 3, **Table 3**).

In contrast, alcohol to oil MR had a positive impact on IMSO ethanolysis regardless of whether the reaction was under kinetic or thermodynamic control (**Figure 4**). The effect is however more significant when operating at a MR limiting value of 6:1. Indeed, at ambient temperature (35°C) while rather similar ester profiles are obtained for MR ≥ 8:1, the deviation is visible for MR = 6:1 by slowing the reaction rate and lowering the plateau of the 1st stage chemical equilibrium (5 wt %, **Figure 4a**). This latter effect is even more important when operating under higher temperature (78°C), with an ester content decrement of 15 wt % observed when the MR decreased from 8:1 to 6:1 (**Figure 4b**). This result may be attributed to the enhanced miscibility of glycerol in the reacting mixture under high temperature; within this context, the relevant option to counterbalance this effect is to add ethanol in higher proportion to shift the chemical equilibrium towards ester production.

Moreover, addition of glycerol involves a progress of the reaction all the more substantial that glyceride conversion is incomplete (ester content increment of 8 wt % reduced to 5 wt % when operating IMSO ethanolysis at 78°C or at 35°C) (**Figure 4**). Therefore for MR = 8:1, addition of glycerol enhanced the plateau of the 2nd stage chemical equilibrium which reached at 78°C the same level as the plateau reached at 35°C (**Figure 3**). Nevertheless, a larger amount of glycerol than 25 wt % (up to 35 wt %) produced no significant rise in the ester content at the 2nd stage (exp. 9, **Table 3**).

As could be expected, catalyst concentration has no effect on the chemical equilibrium plateau, however in large excess it had a negative impact on glyceride conversion, with a slower increment in the ester content after glycerol addition, likely by limiting liquid-liquid demixing of the reacting mixture (exp. 12 vs 11 or 13, **Figure 5**).

The addition of recycled crude glycerol obtained as a by-product from previous biodiesel production batches (ethanolysis & separation) yields as good results as the addition of pure glycerol tested in the original procedure (**Nitièma-Yefanova et al., 2016-2017**) (exp. 2 vs 8; exp. 1 vs 10). Although this result is not surprising, since crude glycerol is rich in catalyst and thus, can only increase even more the oil conversion, the recycling of glycerol is more suitable for industrial purposes.

In addition of showing that the kinetics of ethanolysis is established by the major fatty acid moiety of the departure lipid feedstock (i.e. oleic acid here), the results in **Figure 6** and **Table 3** confirm that the two tested oils, IMSOy and IMSOb, have similar behavior; this is in

compliance with their very close chemical and physical properties (**Tables 1-2**), except for the sulfur content that finally does not induce any difference. Therefore, the ethyl esters produced from the two oils IMSOy and IMSOb will be designated in the following under a single denomination IMSOEEs.

The key parameters of ethanolysis optimized in previous works for NEVOs (*Balanites aegyptiaca* and *Azadirachta* oils (**Nitièma-Yefanova et al., 2016-2017**)) can be used for the IMSOs resulting in similar efficiencies and guaranteeing satisfactory results (exp. 2, **Table 3**). Moreover, the rather successful results obtained at a larger scale (× 3) suggest a satisfactory transfer at pilot scale (exp. 11 vs 13, **Table 3** and **Figure 5**). The recent work carried out on ethanolysis of mustard (*Brassica nigra*) seed oil by using the traditional one-stage procedure with similar operating conditions except for the reaction temperature (60°C) led to much higher content in esters (98 wt %) (**Fadhil et al., 2014**); however, this value was obtained after purification of the produced biodiesel.

3.1.2. Purification of IMSOEEs and fuel properties

The dry-purification yield (defined as Y_i (wt %) = (m_i/m_0)×100 with m_i and m_0 the mass of sample before and after treatment respectively) was 95 ± 1 wt %. Characterization results of the produced IMSOEEs before and after dry-purification, along with of treatment efficiency, are shown in **Table 4** for molecular species and chemical elements. As it can be observed, the selected dry-purification procedure combined with the FIMS as adsorbent shows very good performances. Indeed, the treated sample is concentrated in IMSOEEs with no retention of specific esters while all contaminants are removed in whole (free glycerin, TGs, and K) or in part (MGs, DGs, Sn), with the exception of water. This contamination from the FIMS suggests that likely more care should be taken during storage (with a container tightly closed and protected from moisture). Regarding the residual Sn in the purified IMSOEEs, it would difficult to conclude whether this contamination brought during IMSO extraction by mechanical treatment (**Table 2**) is an issue or not, since no standard-limiting requirement exists to date for this metal. Also, it should be mentioned that the S atomic species initially observed by ICP-AES in the departure IMSO (around 15 ppm on average, **Table 2**) is no longer detected in the crude IMSOEEs; this reveals that the probably responsible glucosinolates are converted (into other molecules than FAEEs) during the IMSO ethanolysis. Occurrence of other species than glycerides (pool convertible into FAEEs) in the departure IMSO may explain the low IMSOEE content obtained prior purification (88 wt %).

Although ester content does not meet the specifications after dry-purification (95.8 instead of the required 96.5 wt %), the resulting IMSOEE product shows very satisfactory physical properties as biodiesel (**Table 6**). This makes it a good candidate to pursue further investigations with thermal and emission analyses and thus get a significant diagnosis.

3.2. Biolubricant production and main performance properties

3.2.1. Reaction

Global results of IMSOEE transesterification with 2E1H for yielding IMSO2E1HEs (biolubricant) are gathered in **Table 5a**. Unfortunately, the cooling system of the vacuum reactive distillation unit has not been efficient enough to trap all ethanol produced during transesterification. Consequently, overall material balance could not be done and **Figure 7** depicts mass fraction vs time profiles for all reaction mixture species except ethanol. The whole results highlights some important points discussed below.

Figure 7

Mass fractions vs time of the reaction mixture species verify the specific features of any reversible reaction under successive kinetic and thermodynamic control, with no mass transfer limitation. Thence, profiles of IMSO2E1HEs and IMSOEEs are very similar (**Figures 7** and **3**).

Furthermore, pressure has clearly a significant impact on IMSOEE transesterification with 2E1H. The lower is the operating pressure, higher is the reaction yield, just as the IMSOEE conversion and IMSO2E1HE mass fraction, if these are considered only at the end of reaction (**Table 5a**).

Nevertheless, when considering evolution vs time, **Figure 7** clearly shows that the chemical equilibrium state of the IMSOEE transesterification with 2E1H is reached faster when increasing pressure, with however a plateau located lower. On the other hand, when the operating pressure is too low, IMSOEE conversion (just as IMSO2E1HE formation) is slower at the early stage of the reaction. This phenomena might be attributed to a partial vaporization of 2E1H during reactive distillation. Indeed, assuming that transesterification of IMSOEEs with 2E1H (**Figure 2**) is of partial first order in each reactant, the initial reaction rate r_0 can be written as (considering that reaction occurs in a closed perfectly stirred reactor of constant volume):

$$r_0 = k_0\,[IMSOEEs]_0\,[2E1H]_0, \tag{3a}$$

$$\text{with } r_0 = \left(\frac{d[IMSO2E1HEs]}{dt}\right)_0 \approx \frac{\Delta[IMSO2E1HEs]}{\Delta t} \quad \text{if} \quad \Delta t \text{ small}, \tag{3b}$$

where k_0 and $[R_i]_0$ are respectively the initial kinetic constant and molar concentration of reactant R_i. Thence, for two IMSOEE transesterification reactions carried out at different pressures (P_2, P_3) all other operating conditions remaining constant, the ratio between their initial reaction rates $r_0^{P_2}/r_0^{P_3}$ attributed to partial evaporation of 2E1H should be equal to $[2E1H]_0^{P_2}/[2E1H]_0^{P_3}$. By taking as initial conditions the reacting mixture composition after 4 min reaction time, we obtain:

$$\left(\frac{\Delta[IMSO2E1HEs]}{\Delta t}\right)^{P_2}/\left(\frac{\Delta[IMSO2E1HEs]}{\Delta t}\right)^{P_3} = 1.08 \quad \text{and} \quad [2E1H]_0^{P_2}/[2E1H]_0^{P_3} = 1.11 \qquad (4)$$

leading to the conclusion that assumption of partial 2E1H vaporization is valid.

Within a different context focused on hydraulic fluid synthesis by enzymatic esterification of fatty acids with a polyol, **Kim et al. (2019)** also observed the importance of applying a suitable vacuum level to reach good yields. Indeed, the issue was to inhibit hydrolysis (by removing water formed during esterification) thanks to a high vacuum but the latter could not be too high in order to keep enough water to ensure a significant enzymatic activity. In a similar context of hydraulic fluid synthesis but here by autocatalytic esterification followed by short-path distillation, **Maurad et al. (2018)** also highlighted the crucial role of vacuum applied in the two stages (500 and 0.05 mbar respectively).

Similarly to the IMSO ethanolysis, kinetics of IMSOEE transesterification with 2E1H is imposed by the major ethyl ester, i.e. ethyl oleate (**Figure 8**).

Figure 8

Moreover, the reactive distillation under low pressure proves to be a relevant option allowing for shifting the chemical equilibrium towards formation of biolubricant by ethanol removal from the reacting mixture and thus improving reaction yield and product purity. Under the optimal pressure of 0.05 bar (other operating conditions: 70°C, MR (2E1H to IMSOEEs) = 2:1, [KOH] = 2 wt %) 93 wt % of the departure IMSOEEs were converted in less than 65 min, with a reaction yield and an IMSO2E1HE content of respectively 91 and 71 wt % (**Table 5a**). Here again, it should be noted that a higher content in IMSO2E1HEs would have been obtained if the departure IMSO had been pre-treated to increase the glyceride pool, and thus the IMSOEE content.

551 *3.2.2. Purification of IMSO2E1HEs and lubricant properties*

552 In order to simulate a worst case, efficiency of the purification method was evaluated
553 by selecting the sample of IMSO2E1HEs showing a poor content in esters (63.8 wt % obtained
554 under the reaction pressure of 0.10 bar).

555 As illustrated in **Table 5b**, purification of IMSO2E1HEs shows very good performance
556 once the catalyst is removed through bubble-washing and the excess of 2-ethyl-1-hexanol
557 (including the residual ethanol traces) through vacuum distillation. All esters are thus more
558 concentrated in the residue, of which the non-converted IMSOEEs could not be removed
559 successfully under 0.01 bar (minimum operating pressure reached with the equipment used).

560 Nevertheless, the resulting IMSO2E1HE product shows satisfactory behavior as
561 biolubricant (**Table 6**), at least regarding the basic properties (density, viscosity, and color)
562 **(Habib et al., 2014; Trivedi et al., 2015; McNutt and He, 2016; Zheng et al., 2018)**. The
563 higher color Gardner observed for the IMSO2E1HEs compared with the RO2E1HEs is due to
564 the parent oil (orange for the IMSO, pale yellow for rapeseed oil RO). Moreover, the high acid
565 value of the IMSO2E1HE product might be reduced by operating with a less concentrated citric
566 acid solution during bubble-washing. This change should not be prejudicial thanks to the
567 demonstrated driving force efficiency of citric acid in removing the catalyst in the form of
568 potassium citrate. The remaining traces of citric acid should not be prejudicial either since the
569 addition of this natural antioxidant proved to enhance the oxidation stability of biolubricants
570 **(Sharma et al., 2016)**, similarly to biodiesel and vegetable oils **(Serrano et al., 2013; Yaakob**
571 **et al., 2014; Bekkar et al., 2018)**. This could also compensate for the rather high content of
572 polyunsaturated species encountered in the produced IMSO2E1HEs (linoleic and linolenic
573 esters: 37 wt %) compared to monounsaturated ones (46 wt %), containing however oleic like
574 esters in large part (35 wt %) (**Table 5b**). Indeed, a low degree of unsaturation is preferred for
575 better thermal-oxidative stability, as well as higher viscosity; however, it is also desirable to
576 keep a certain number of unsaturation sites to meet suitable cold flow properties. Moreover, an
577 increase in the fatty chain length increases the viscosity. Thence, high oleic acid vegetable oils
578 are considered optimal to produce high performance biolubricants **(Reeves et al., 2015; Chan**
579 **et al., 2018)**. Thermal-oxidative stability of the produced IMSO2E1HEs could not be evaluated
580 in this work. Nonetheless, the obtained viscosity meeting the requirements (for metalworking
581 fluids), it can be assumed that the effect of the polyunsaturated esters (linoleic and linolenic
582 acid esters) is counter-balanced by the presence of monounsaturated longer chain esters (C20
583 to C22) (**Tables 5b-6**). Furthermore, should viscosity of the obtained IMSO2E1HE product
584 need to be enhanced for a specific application, ethyl cellulose (EC) which is able to boost this

property by two-fold in small amounts could be used as additive (**Chan et al., 2018**). Additionally, EC could be derived from Indian mustard stems rich in cellulose (**Rapp et al., 2018**), which would broaden even more the contours of a biorefinery system focused on Indian mustard. Finally, it was observed that transesterification of fatty acid methyl esters with 2-ethyl-1-hexanol instead of trimethylolpropane led to a biolubricant showing better cold flow properties and, moreover, in a shorter reaction time (**McNutt et al., 2016**). As a result, all these considerations suggest that the obtained IMSO2E1HE product is a potential candidate as biolubricant, particularly as a metalworking fluid.

Table 6

4. Conclusions

The two routes investigated in this work for harnessing IMSO as an energy carrier (IMSOEEs) or biolubricant (IMSO2E1HEs) via conversion of IMSOEEs led to positive results.

Although based on homogeneous catalysis, the alkali route selected for IMSO conversion into IMSOEEs leads to an interesting alternative of low cost production of a 100% renewable biodiesel. The main features of this alternative are firstly, simple operating conditions (35°C, atmospheric pressure, ethanol to oil molar ratio of 8, 1.1 wt % KOH, 50 min); and secondly, a two-stage procedure based on glycerol recycling followed by a dry-purification method based on Indian mustard stems (FIMS). Moreover, a satisfactory ester content was reached (95.8 wt %) and the produced IMSOEEs subsequently met the basic biodiesel properties (acid value, color, density, viscosity, flash point, pour point, cloud point, and cold filter plugging point). Nevertheless, a pre-treatment of the departure IMSO prior ethanolysis would be beneficial by removing species that are not glycerides, such as glucosinolates, and thus ensuring the produced biodiesel conforms to industry specifications (such as EN 14214 standard).

Regarding the IMSO2E1HE production via transesterification of unpurified IMSOEEs with 2E1H, the selection of reactive distillation with optimized operating pressure (0.05 bar, at 70°C with 2 wt % of KOH and a 2E1H to IMSOEEs molar ratio of 2 in 65 min) allowed a high conversion of IMSOEEs (93 wt %) to be reached and a IMSO2E1HE content of 71 wt %. However, the latter value could be improved by increasing the glyceride pool of the parent IMSO, and thus the ester content of the departure IMSOEEs. Nonetheless, after purification by bubble-washing (driven by citric acid) and vacuum distillation (inferior to 0.01 bar), the

resulting IMSO2E1HE product exhibited interesting basic properties (density, viscosity, and color) making it a good biolubricant candidate.

Author contributions

Jing Chen and Xiaoqiang Bian (executing of the biodiesel and biolubricant synthesis); Graeme Rapp and Richard Trethowan (providing of the Indian mustard seeds, oil, and stems; review of the manuscript); James Lang and Alejandro Montoya (Indian mustard oil analysis by GC; review of the manuscript); Brice Bouyssiere (biodiesel analysis by ICP-AES); Jean-François Portha (biolubricant purification and review of the manuscript); Jean-Noël Jaubert (financial support); Peter Pratt (analysis of biodiesel and biolubricant specific properties); Lucie Coniglio (conceptualization, methodology, assistance during biodiesel and biolubricant production, and writing of the manuscript).

Acknowledgments

The authors are very appreciative to Frédéric Roze and Jean-François Remy for their technical support and to Dr. Olivier Herbinet, Professor Véronique Falk and Professor Raphaël Schneider for their helpful discussions during the work (members of Université de Lorraine - Ecole Nationale Supérieure des Industries Chimiques de Nancy, Laboratoire Réactions et Génie des Procédés UMR CNRS 7274, 54001 Nancy Cedex, France).

References

ASTM D1544-04(2010), Standard Test Method for Color of Transparent Liquids (Gardner Color Scale), ASTM International, West Conshohocken, PA, 2010.

ASTM D1983-90(1995)e1, Standard Test Method for Fatty Acid Composition by Gas-Liquid Chromatography of Methyl Esters (Withdrawn 2003), ASTM International, West Conshohocken, PA, 1995.

Bekkar, K, Oumeddour, R., Nigri, S., Selaimia, R., 2018. Improved stability to auto-oxidation of the olive oil by addition of citric acid. Emir. J. Food Agr. 30, 621-630. http://www.ejfa.me/10.9755/ejfa.2018.v30.i7.1749.

651 Berrios, M., Martín, M.A., Chica, A.F., Martín, A., 2011. Purification of biodiesel from used
652 cooking oils. Appl. Energy 88, 3625-3631.
653 https://doi.org/10.1016/j.apenergy.2011.04.060.
654 Bolonio, D., Llamas, A., Rodríguez-Fernández, J., Al-Lal, A.M., Canoira, L., Lapuerta, M.,
655 Gómez, L., 2015. Estimation of Cold Flow Performance and Oxidation Stability of Fatty
656 Acid Ethyl Esters from Lipids Obtained from Escherichia coli. Energy Fuels 29, 2493-
657 2502. https://doi.org/10.1021/acs.energyfuels.5b00141.
658 Boomiraj, K., Chakrabarti, B., Aggarwal, P.K., Choudhary, R., Chander, S., 2010. Assessing
659 the vulnerability of Indian mustard to climate change. Agric. Ecosyst. Environ. 138, 265-
660 273. https://doi.org/10.1016/j.agee.2010.05.010.
661 Brunschwig, C., Moussavou, W., Blin, J., 2012. Use of bioethanol for biodiesel production.
662 Prog. Energy Combust. Sci. 38, 283-301. https://doi.org/10.1016/j.pecs.2011.11.001.
663 Carareto, N.D.D., Kimura, C.Y.C.S., Oliveira, E.C., Costa, M.C., Meirelles, A.J.A., 2012. Flash
664 points of mixtures containing ethyl or ethylic biodiesel and ethanol. Fuel 96, 319-326.
665 https://doi.org/10.1016/j.fuel.2012.01.025.
666 Caumette, G., Lienemann, C.P., Merdrignac, I., Bouyssiere, B., Lobinski, R., 2010.
667 Fractionation and speciation of nickel and vanadium in crude oils by size exclusion
668 chromatography-ICP MS and normal phase HPLC-ICP MS. J. Anal. At. Spectrom. 25,
669 1123-1129. http://dx.doi.org/10.1039/c003455j.
670 Cermak, S.C., Bredsguard, J.B., John, B.L., McCalvin, J.S., Thompsonb, T., Isbell, K.N.,
671 Feken, K.A., Isbell, T.A., Rex E. Murray, R.E., 2013. Synthesis and physical properties
672 of new estolide esters. Ind. Crop. Prod. 46, 386-391.
673 http://dx.doi.org/10.1016/j.indcrop.2013.02.006.
674 Cerón, A.A., Vilas Boas, R.N., Biaggio, F.C. de Castro, H.F., 2018. Synthesis of biolubricant
675 by transesterification of palm kernel oil with simulated fusel oil: Batch and continuous
676 processes. Biomass Bioenergy 119, 166-172.
677 https://doi.org/10.1016/j.biombioe.2018.09.013
678 Chan, C.H., Tang, S.W., Mohd, N.K., Lim, W.H., Yeong, S.K., Idris, Z., 2018. Tribological
679 behavior of biolubricant base stocks and additives. Renew. Sust. Energy Rev. 93, 145-
680 157. https://doi.org/10.1016/j.rser.2018.05.024.
681 Coniglio, L., Bennadji, H., Glaude, P.A., Herbinet, O., Billaud, F., 2013. Combustion chemical
682 kinetics of biodiesel and related compounds (methyl and ethyl esters): Experiments and
683 modeling Advances and future refinements. Prog. Energy Combust. Sci. 39, 340-382.
684 http://dx.doi.org/10.1016/j.pecs.2013.03.002.

685 Coniglio, L., Coutinho, J.A.P., Clavier, J.Y., Jolibert, F., Jose, J., Mokbel, I., Pillot, D., Pons,
686 M.N., Sergent, M., Tschamber, V., 2014. Biodiesel via supercritical ethanolysis within a
687 global analysis "feedstocks-conversion-engine" for a sustainable fuel alternative. Prog.
688 Energy Combust. Sci. 43, 1-35. http://dx.doi.org/10.1016/j.pecs.2014.03.001.
689 de Haro, J.C. del Prado Garrido, M., Pérez, À., Carmona, M., Rodríguez, J.F., Full conversion
690 of oleic acid to estolides esters, biodiesel and choline carboxylates in three easy steps. J.
691 Clean. Prod. 184, 579-585. https://doi.org/10.1016/j.jclepro.2018.02.190.
692 EN-14103, Fat and oil derivatives, Fatty Acid Methyl esters (FAME) - Determination of ester
693 and linoleic acid methyl ester contents, European Committee for Standardization,
694 Brussels (Belgium), 2011.
695 EN-14104, Fat and oil derivatives, Fatty Acid Methyl Esters (FAME) - Determination of acid
696 value, European Committee for Standardization, Brussels (Belgium), 2003.
697 EN-14105, Fat and oil derivatives, Fatty Acid Methyl Esters (FAME) - Determination of free
698 and total glycerol and mono-, di-, triglyceride contents, European Committee for
699 Standardization, Brussels (Belgium), 2011.
700 EN-ISO-12185, Crude petroleum and petroleum products - Determination of density -
701 Oscillating U-tube method, European Committee for Standardization, Brussels
702 (Belgium), 1996.
703 EN-ISO-12937, Petroleum products - Determination of water - Coulometric Karl Fischer
704 titration method, European Committee for Standardization, Brussels (Belgium), 2000.
705 EN-ISO-3104, Petroleum products - Transparent and opaque liquids - Determination of
706 kinematic viscosity and calculation of dynamic viscosity, European Committee for
707 Standardization, Brussels (Belgium), 1996.
708 Fadhil, B., Abdelrahman, S., Waseem, A., 2014. Transesterification of mustard (*Brassica*
709 *nigra*) seed oil with ethanol: Purification of the crude ethyl ester with activated carbon
710 produced from de-oiled cake. Energy Convers. Manag. 77, 495-503.
711 http://dx.doi.org/10.1016/j.enconman.2013.10.008.
712 Feng, Z., Odelius, K., Rajarao, G.K., Hakkarainen, M., 2018. Microwave carbonized cellulose
713 for trace pharmaceutical adsorption. Chem. Eng. J. 346, 557-566.
714 https://doi.org/10.1016/j.cej.2018.04.014.
715 Geethanjali, G., Padmaja, K.V., Prasad, R.B. N., 2016. Synthesis, Characterization, and
716 Evaluation of Castor Oil-Based Acylated Derivatives as Potential Lubricant Base Stocks.
717 Ind. Eng. Chem. Res. 55, 9109-9117. https://doi.org/10.1021/acs.iecr.6b01550.

718 Habib, N.S.H.A., Yunus, R., Rashid, U., Taufiq-Yap, Y.H., Abidin, Z.Z., Syam, A.M., Irawan,
719 S., 2014. Transesterification reaction for synthesis of palm-based ethylhexyl ester and
720 formulation as base oil for synthetic drilling fluid. J. Oleo Sci. 63, 497-506.
721 https://doi.org/10.5650/jos.ess13220.
722 Handiseni, M., Brown, J., Zemetra, R., Mazzola, M., 2012. Use of Brassicaceous seed meals to
723 improve seedling emergence of tomato and pepper in Pythium ultimum infested soils.
724 Arch. Phytopathol. Plant Protect. 45, 1204-1209.
725 https://doi.org/10.1080/03235408.2012.660611.
726 Hossain Md. Anwar, Mohammad Anwar Mohamed Iqbal, Nurhidayatullaili Muhd Julkapli, Pei
727 San Kong, Juan Joon Ching, Hwei Voon Lee, 2018. Development of catalyst complexes
728 for upgrading biomass into ester-based biolubricants for automotive applications: a
729 review. RSC Adv. 8, 5559-5577. https://doi.org/10.1039/c7ra11824d.
730 Ineos Enterprises France, Verdun, France, 2018, Private communication.
731 ISO-6618, Petroleum products and lubricants - Determination of acid or base number - Colour
732 indicator titration method, Technical committee ISO/TC 28 Petroleum products and
733 lubricants, 1997.
734 Karmakar, G., Ghosh, P., Sharma, B.K., 2017. Chemically Modifying Vegetable Oils to Prepare
735 Green Lubricants. Lubricants 5, 44-61. https://doi.org/10.3390/lubricants5040044.
736 Kim, H., Choi, N., Kim, Y., Kim, H.R., Lee, J., Kim, I.-H., Immobilized lipase-catalyzed
737 esterification for synthesis of trimethylolpropane triester as a biolubricant. Renew.
738 Energy 130, 489-494. https://doi.org/10.1016/j.renene.2018.06.092.
739 Kirkegaard, J.A., Sarwar, M., 1999. Glucosinolate profiles of Australian canola (*Brassica*
740 *napus annua L.*) and Indian mustard (*Brassica juncea L.*) cultivars: implications for
741 biofumigation. Aust. J. Agric. Res. 50, 315-324. https://doi.org/10.1071/A98124.
742 Kleinaitė, E., Jaška, V., Tvaska, B., Matijošytė, I., 2014. A cleaner approach for biolubricant
743 production using biodiesel as a starting material. J. Clean Prod. 75, 40-44.
744 https://doi.org/10.1016/j.jclepro.2014.03.077.
745 Maurad, Z.A., Yeong, S.K., Idris, Z., Ishak, S.A., 2018. Combined esterification and short-path
746 distillation for high-purity pentaerythritol ester from palm kernel for biolubricants. J. Am.
747 Oil Chem. Soc. 95, 1421-1429. https://doi.org/10.1002/aocs.12149.
748 Mazivila, S.J., Mitsutake, H., de Santana, F.B., Gontijo, L.C., Santos, D.Q., Neto, W.B., 2015.
749 Fast classification of different oils and routes used in biodiesel production using mid
750 infrared spectroscopy and PLS2-DA. J. Braz. Chem. Soc. 26, 642-648.
751 http://dx.doi.org/10.5935/0103-5053.20150020.

McNutt, J., He, Q.S., 2016. Development of biolubricants from vegetable oils via chemical modification. J. Ind. Eng. Chem. 36, 1-12. http://dx.doi.org/10.1016/j.jiec.2016.02.008.

Muhammad, F., Oliveira, M.B., Pignat, P., Jaubert, J-N., Pinho, S.P., Coniglio, L., 2017. Phase equilibrium data and modeling of ethylic biodiesel, with application to a non-edible vegetable oil. Fuel. 203, 633-641. https://doi.org/10.1016/j.fuel.2017.05.007.

Navarro-Pineda, F.S., Baz-Rodríguez, S.A., Handler, R., Sacramento-Rivero, J.C., 2016. Advances on the processing of *Jatropha curcas* towards a whole-crop biorefinery. Renew. Sust. Energy Rev. 54, 247-269. https://doi.org/10.1016/j.rser.2015.10.009.

Ngala, B.M., Haydock, P.P.J., Woods, S., Back, M.A., 2015. Biofumigation with *Brassica juncea*, *Raphanus sativus* and *Eruca sativa* for the management of field populations of the potato cyst nematode Globodera pallida. Pest Manag. Sci. 71, 759-769. https://doi.org/10.1002/ps.3849.

Nitièma-Yefanova, S., Coniglio, L., Schneider, R., Nébié, R.H.C., Bonzi-Coulibaly, Y.L., 2016. Ethyl biodiesel production from non-edible oils of *Balanites aegyptiaca*, *Azadirachta indica*, and *Jatropha curcas* seeds – Laboratory scale development. Renew. Energy 96, 881-890. http://dx.doi.org/10.1016/j.renene.2016.04.100.

Nitièma-Yefanova, S., Richard, R., Thiebaud-Roux, S., Bouyssiere, B., Bonzi-Coulibaly, Y.L., Nébié, R.H., Mozet, K., Coniglio, L., 2015. Dry-purification by natural adsorbents of ethyl biodiesels derived from nonedible oils. Energy Fuels 29, 150-159. https://doi.org/10.1021/ef501365u.

Nitièma-Yefanova, S., Tschamber, V., Richard, R., Thiebaud-Roux, S., Bouyssiere, B., Bonzi-Coulibaly, Y.L., Nébié, R.H.C., Coniglio, L., 2017. Ethyl biodiesels derived from non-edible oils within the biorefinery concept – Pilot scale production & engine emissions. Renew. Energy 109, 634-645. http://dx.doi.org/10.1016/j.renene.2017.03.058.

Panchal, T.M., Patel, A., Chauhan, D.D., Thomas, M., Patel, J.V., 2017. A methodological review on bio-lubricants from vegetable oil based resources. Renew. Sust. Energy Rev. 70, 65-70. http://dx.doi.org/10.1016/j.rser.2016.11.105.

Pohl, P., Vorapalawut, N., Bouyssiere, B., Carrier, H., Lobinski, R., 2010. Direct multi-element analysis of crude oils and gas condensates by double-focusing sector field inductively coupled plasma mass spectrometry (ICP MS). J. Anal. At. Spectrom. 25, 704-709. http://dx.doi.org/10.1039/c000658k.

Raman, J.K., Alves, C.M., Gnansounou, E., 2018. A review on moringa tree and vetiver grass -Potential biorefinery feedstocks. Bioresour. Technol. 249, 1044-1051. https://doi.org/10.1016/j.biortech.2017.10.094.

786 Rapp, G., 2018. The value of Indian mustard in cereal and legume crop sequences in northwest
787 NSW. Master Thesis, University of Sydney, Australia. http://hdl.handle.net/2123/18504.
788 Rapp, G., Garcia-Montoto, V., Bouyssiere, B., Thiebaud-Roux, S., Montoya, A., Trethowan,
789 R., Pratt, P., Mozet, K., Dufour, A., Coniglio, L., 2018. Dry-purification by natural
790 adsorbents of Indian mustard seed oil ethyl biodiesel and biolubricants: towards a low-
791 cost and environmentally-friendly production route. Private communication.
792 Reeves, C.J., Menezes, P.L., Jen, T.C., Lovell, M.R., 2015. The influence of fatty acids on
793 tribological and thermal properties of natural oils as sustainable biolubricants. Tribol. Int.
794 90, 123-134. http://dx.doi.org/10.1016/j.triboint.2015.04.021.
795 Richard, R., Thiebaud-Roux, S., Prat, L., 2013. Modelling the kinetics of transesterification
796 reaction of sunflower oil with ethanol in microreactors. Chem. Eng. Sci. 87, 258-269.
797 http://dx.doi.org/10.1016/j.ces.2012.10.014.
798 Syahir, A.Z., Zulkifli, N.W.M, Masjuki, H.H., Kalam, M.A., Alabdulkarem, A., Gulzar, M.,
799 Khuong, L.S., Harith, M.H., 2017. A review on bio-based lubricants and their
800 applications, J. Clean. Prod. 168, 997-1016.
801 https://doi.org/10.1016/j.jclepro.2017.09.106.
802 Serrano, M, Bouaid, A., Martinez, M., Araci, J., 2013. Oxidation stability of biodiesel from
803 different feedstocks: Influence of commercial additives and purification step. Fuel 113,
804 50-58. http://dx.doi.org/10.1016/j.fuel.2013.05.078.
805 Sharma, B.K., Biresaw, G., 2016. Environmentally friendly and biobased lubricants, First ed.
806 CRC Press Taylor & Francis Group. ISBN 9781482232028.
807 Singh, V.V., Garg, P., Meena, H.S., Meena, M.L., 2018. Drought Stress Response of Indian
808 Mustard (*Brassica juncea L.*) Genotypes. Int. J. Curr. Microbiol. App. Sci. 7, 2519-2526.
809 https://doi.org/10.20546/ijcmas.2018.703.291.
810 Tabtabaei, S., Boocock, D.G.B., Diosady, L.L., 2014. Biodiesel Feedstock from Emulsions
811 Produced by Aqueous Processing of Yellow Mustard, J. Am. Oil Chem. Soc. 91, 1269-
812 1282. https://doi-org.bases-doc.univ-lorraine.fr/10.1007/s11746-014-2448-8.
813 Trivedi, J., Aila, M., Sharma, C.D., Gupta, P., Kaul, S., 2015. Clean synthesis of biolubricant
814 range esters using novel liquid lipase enzyme in solvent free medium. Springerplus 4, 1-
815 9. https://doi.org/10.1186/s40064-015-0937-3.
816 Yaakob, Z., Narayanan, B.N., Padikkaparambil, S., Unni, S.K., Akbar, M.P., 2014. A review
817 of the oxidation stability of biodiesel. Renew. Sust. Energy Rev. 35, 136-153.
818 http://dx.doi.org/10.1016/j.rser.2014.03.055.

819 Zheng, T., Wu, Z., Xie, Q., Lu, M., Xia, F., Wang, G., Nie, Y., Ji, J., 2018. Biolubricant
820 Production of 2-Ethylhexyl Palmitate by Transesterification Over Unsupported
821 Potassium Carbonate. J. Am. Oil Chem. Soc. 95, 79-88.
822 https://doi.org/10.1002/aocs.12023.
823 Zhou, W., Boocock, D.G.B., 2006. Phase distributions of alcohol, glycerol, and catalyst in the
824 transesterification of soybean oil. J. Am. Oil Chem. Soc. 83, 1041-1045.
825 https://doi.org/10.1007/s11746-006-5161-4.
826

FIGURES

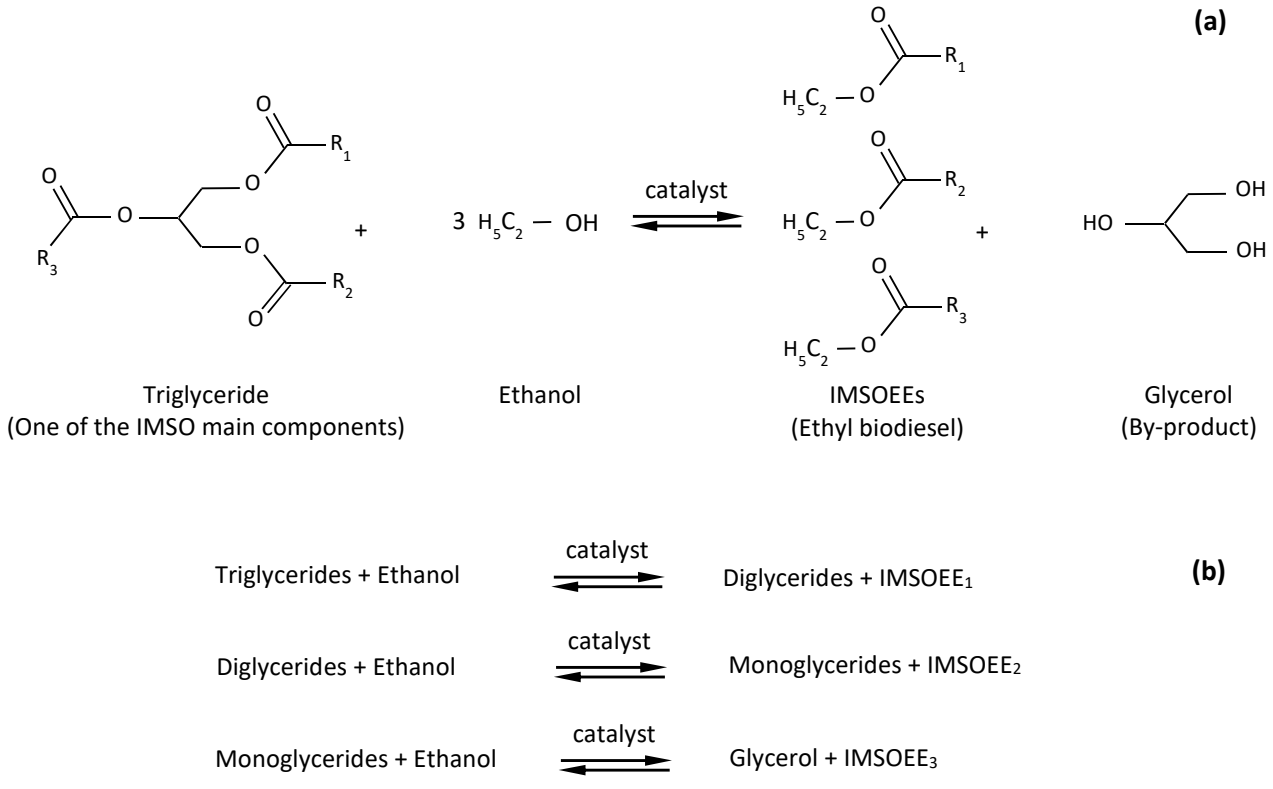

where the active species is $[C_2H_5O^-, K^+]$ when KOH is selected as catalyst.

Figure 1. Catalyzed transesterification reaction of triglycerides involved in IMSO conversion to ethyl biodiesel. **(a)** Overall chemical equation of triglyceride ethanolysis yielding IMSOEEs and glycerol (R_1, R_2, R_3 are identical or different aliphatic chains with zero to three unsaturated bond(s): CH_3-$(CH_2)_m$-$(CH_2$-$CH{=}CH)_n$-$(CH_2)_k$ with $(m+k)$ ranging from 15 to 18 and n = 0, 1, 2 or 3). **(b)** Ethanolysis of triglycerides as a sequence of three consecutive and reversible reactions ($IMSOEE_1$, $IMSOEE_2$, or $IMSOEE_3$ are identical or most likely different). Stoichiometry of the overall reaction (a): 1 mole of triglyceride for 3 moles of ethanol.

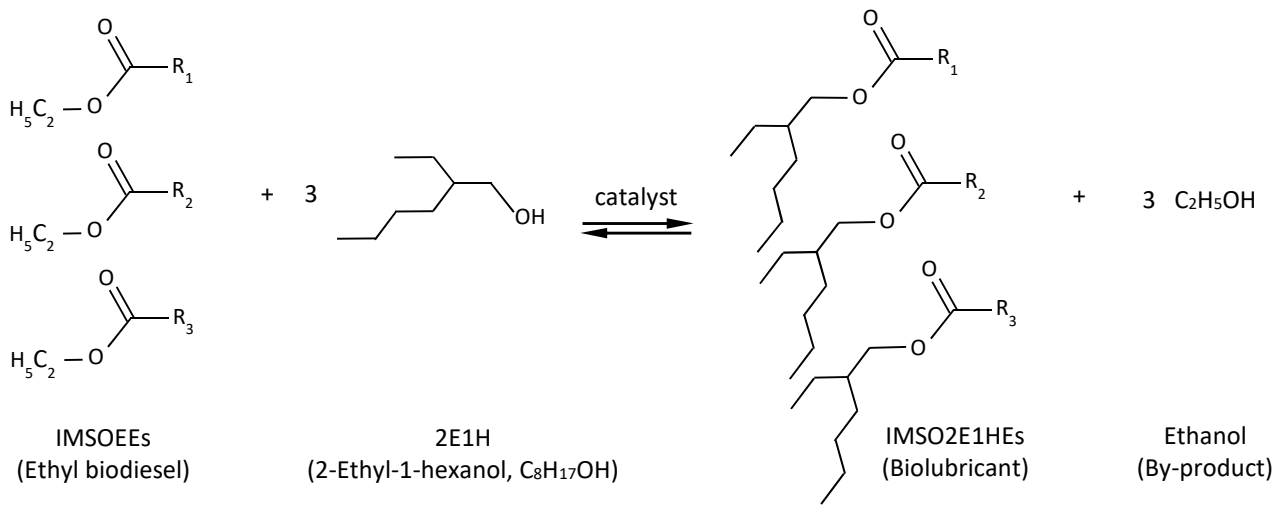

where the active species is $[C_8H_{17}O^-, K^+]$ when KOH is selected as catalyst.

Figure 2. Catalyzed transesterification reaction of IMSOEEs (ethyl biodiesel) with 2-ethyl-1-hexanol (2E1H) yielding IMSO2E1HEs (biolubricant). R_1, R_2, R_3 are different aliphatic chains with zero to three unsaturated bond(s): CH_3-$(CH_2)_m$-$(CH_2$-$CH{=}CH)_n$-$(CH_2)_k$ with $(m+k)$ ranging from 15 to 18 and n = 0, 1, 2 or 3. Stoichiometry of the reaction: 1 mole of IMSOEE for 1 mole of 2E1H.

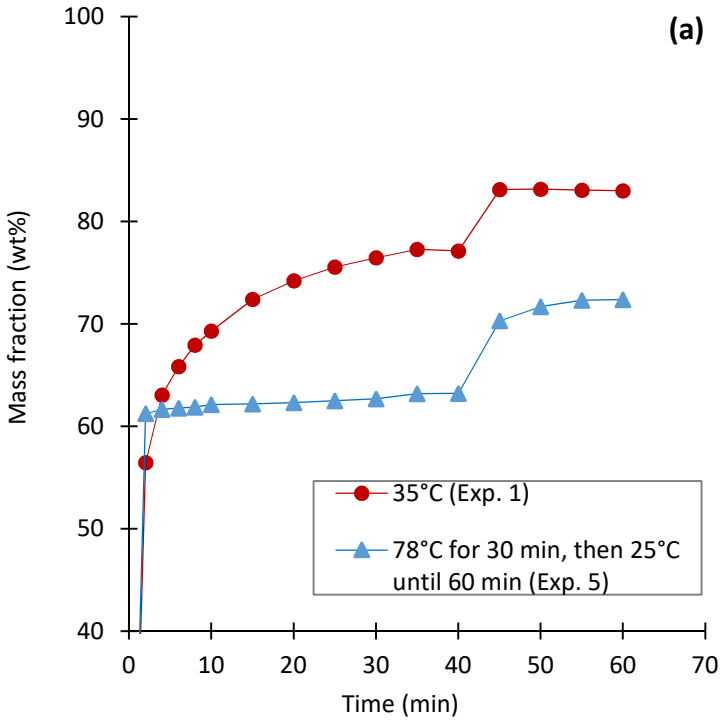

878

879

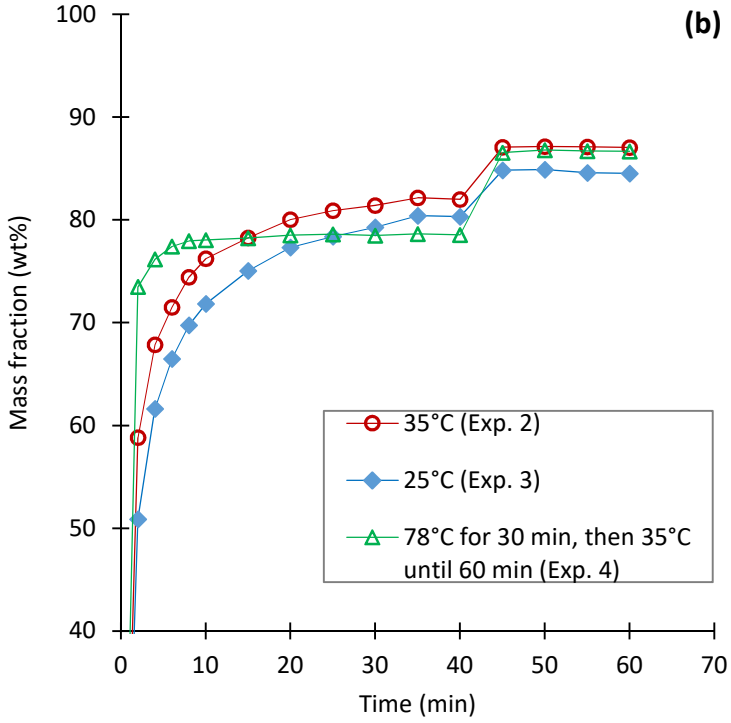

880

881

882 **Figure 3.** IMSOyEE mass fractions as a function of reaction time at different reaction
883 temperature (mass fraction of pure glycerol added: 25 wt %); **(a)** MR (ethanol to oil) = 6, **(b)**
884 MR (ethanol to oil) = 8.

885

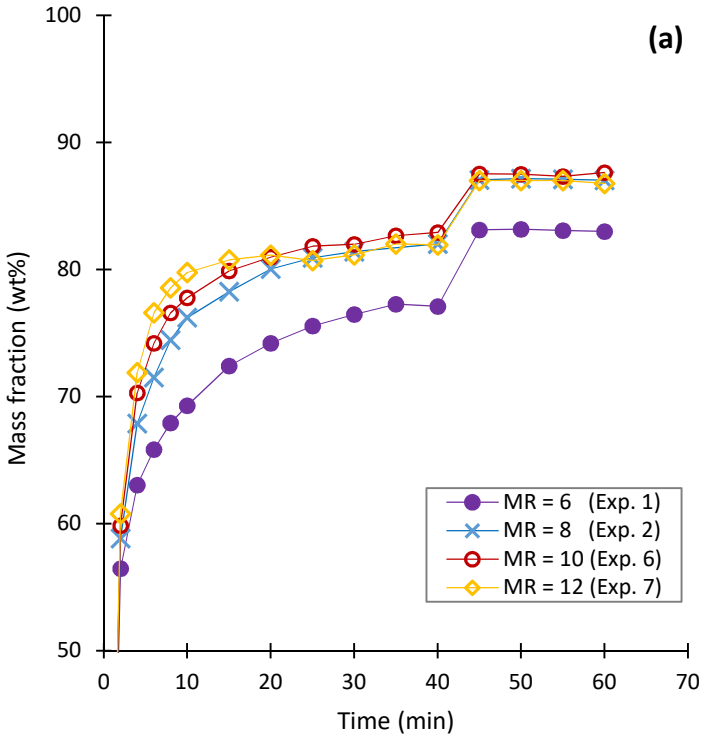

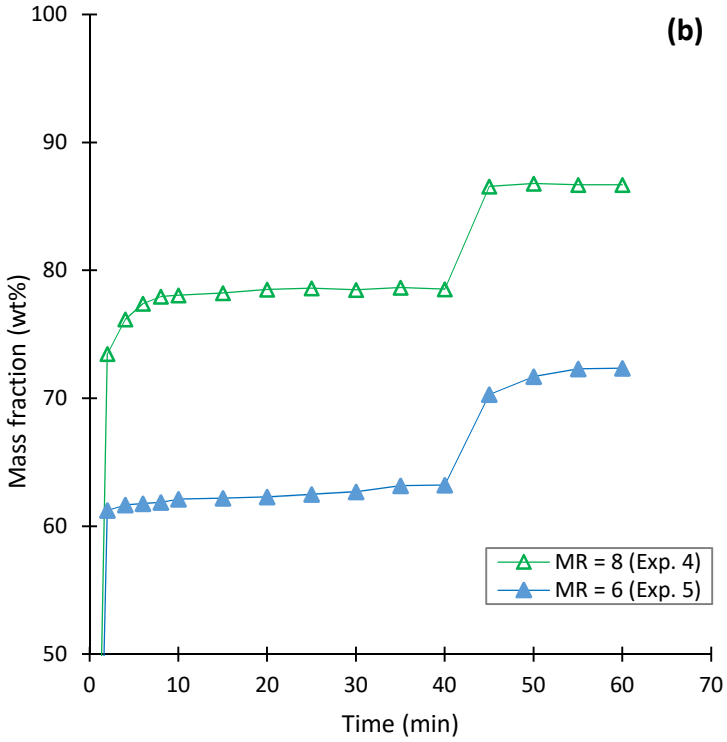

Figure 4. IMSOyEE mass fractions as a function of reaction time at different ethanol to oil molar ratio (MR) (mass fraction of pure glycerol added: 25 wt %); **(a)** 35°C, **(b)** 78°C for 30 min, then 35°C (Exp. 4) or 25°C (Exp. 5) until 60 min.

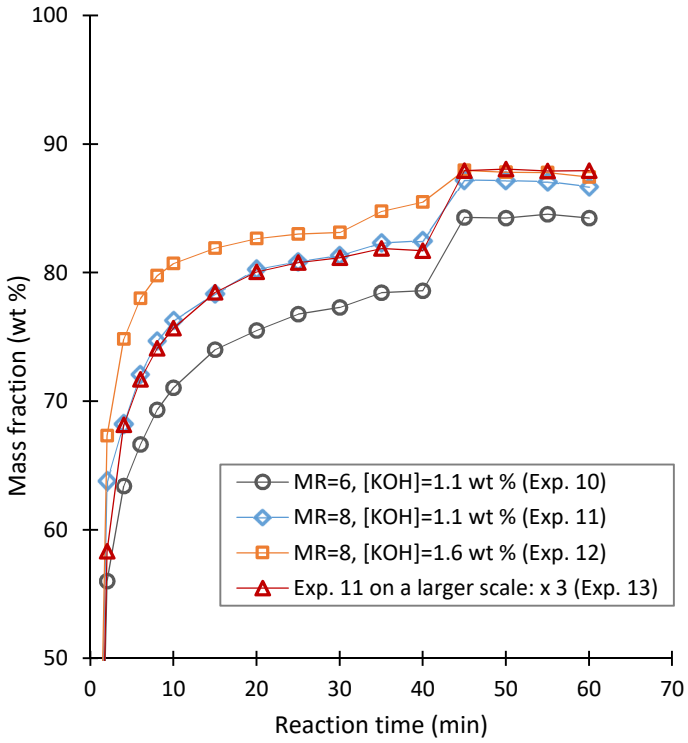

Figure 5. IMSObEE mass fractions as a function of reaction time for different key parameters analyzed separately: ethanol to oil molar ratio (MR), KOH concentration, and a larger scale of reactor (×3) for a given reaction temperature of 35°C (mass fraction of recycled glycerol added: 25 wt %).

902

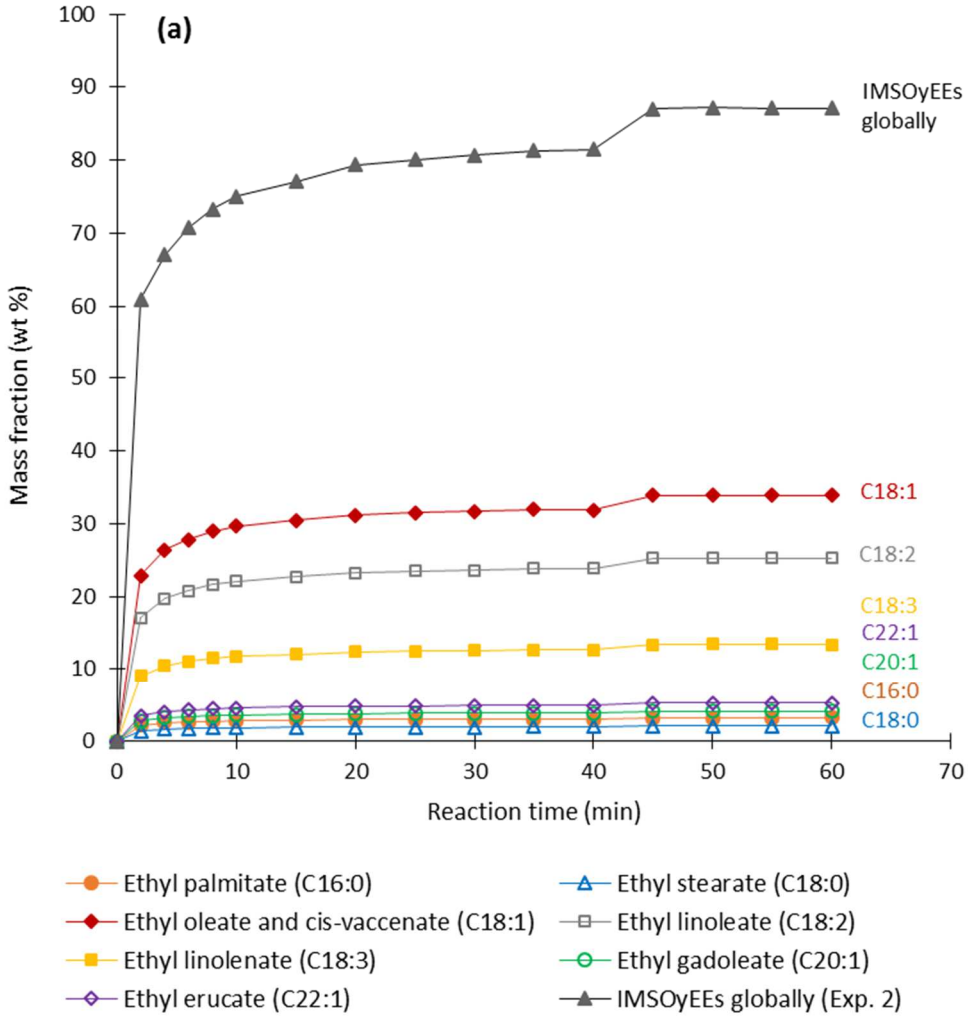
(a)
Mass fraction (wt %)
Reaction time (min)
IMSOyEEs globally
C18:1
C18:2
C18:3
C22:1
C20:1
C16:0
C18:0
Ethyl palmitate (C16:0)
Ethyl stearate (C18:0)
Ethyl oleate and cis-vaccenate (C18:1)
Ethyl linoleate (C18:2)
Ethyl linolenate (C18:3)
Ethyl gadoleate (C20:1)
Ethyl erucate (C22:1)
IMSOyEEs globally (Exp. 2)

903

904

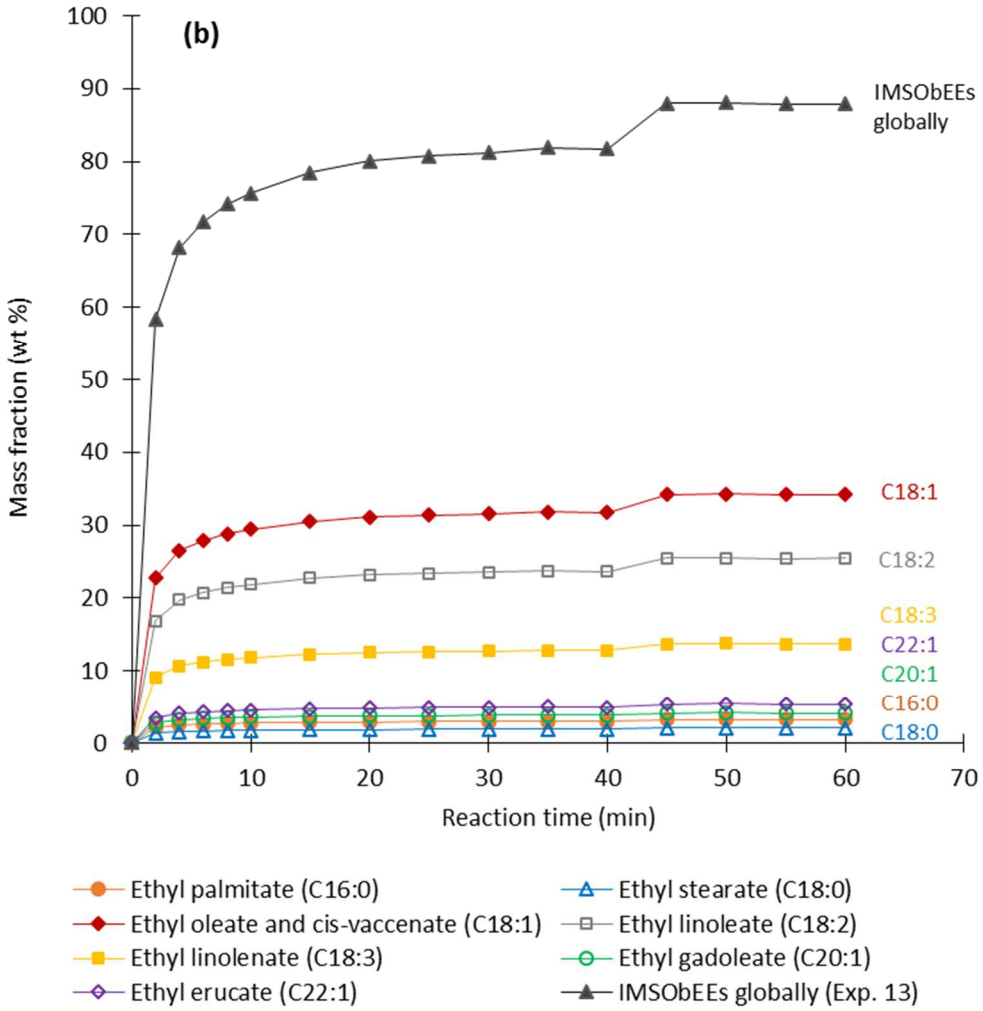

Figure 6. IMSOEE mass fractions as a function of reaction time **(a)** Results for IMSOyEEs globally and distribution of major IMSOyEEs (Exp. 2), **(b)** Results for IMSObEEs globally and distribution of major IMSObEEs (Exp. 13).

912

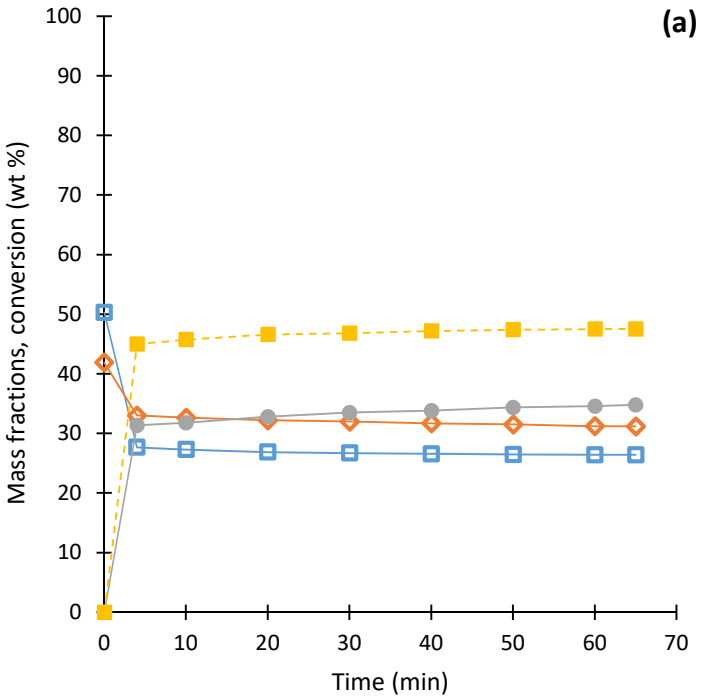

913

914

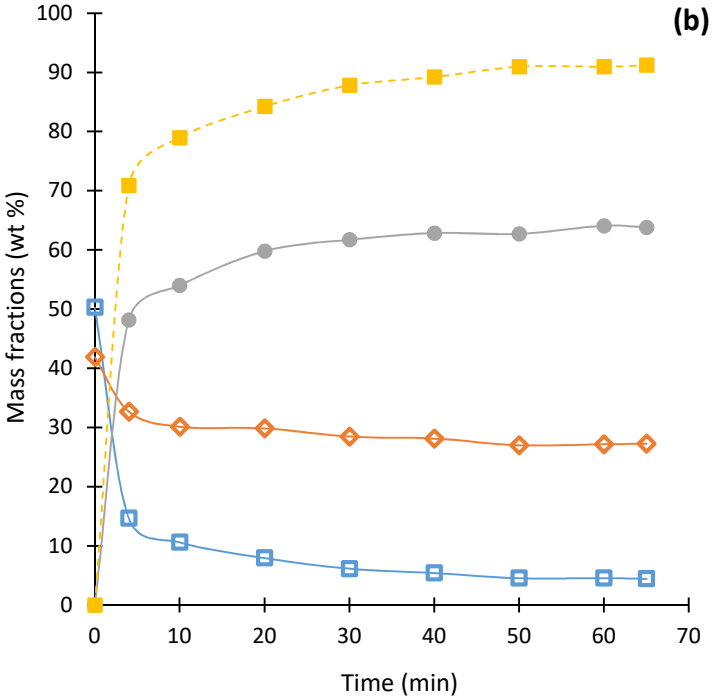

915

916

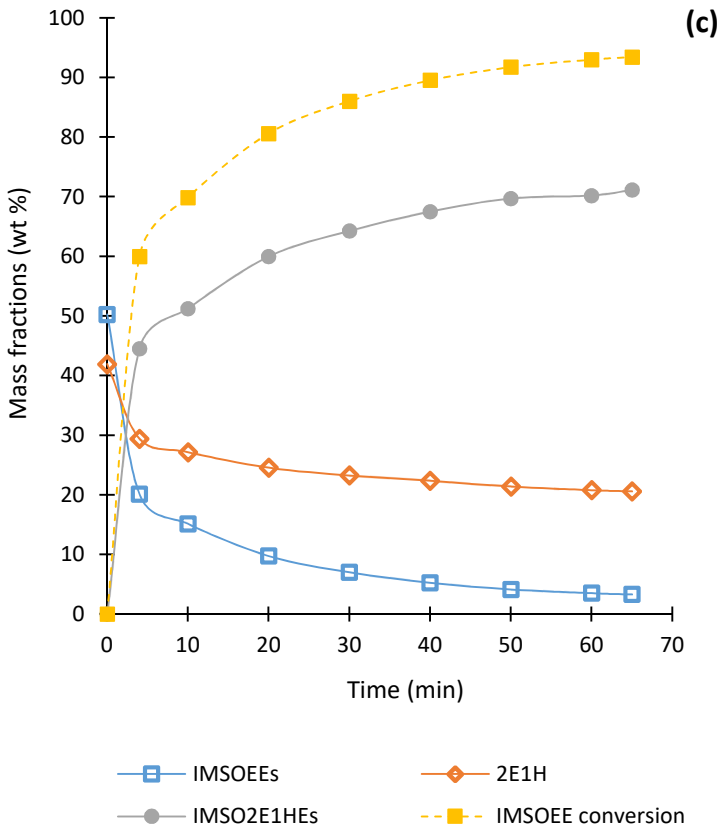

Figure 7. Species mass fractions and conversion as a function of time during transesterification of crude ethyl biodiesel (IMSOEEs) to biolubricant (IMSO2E1HEs). Operating conditions: 70°C, [KOH] = 2 wt %, MR (2E1H to IMSOEEs) = 2, and pressure (in bar) = 0.5 **(a)**, 0.1 **(b)**, 0.05 **(c)**. The residual KOH content due to previous IMSO conversion into IMSOEEs was not included.

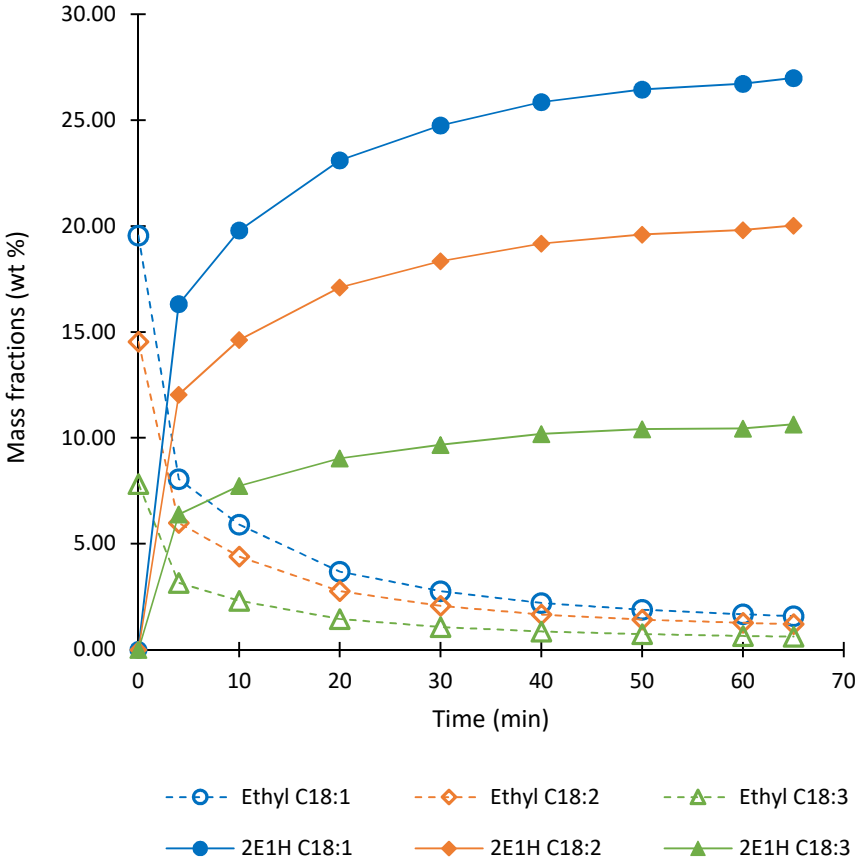

925

926

927 **Figure 8.** Major ester species mass fractions as a function of time during transesterification of
928 crude ethyl biodiesel (IMSOEEs) to biolubricant (IMSO2E1HEs). Operating conditions: 70°C,
929 [KOH] = 2 wt %, MR (2E1H to IMSOEEs) = 2, and pressure (in bar) = 0.05. The residual KOH
930 content due to previous IMSO conversion into IMSOEEs was not included.

931

TABLES

Table 1. Fatty acid composition (molar fractions %) of the IMSOy and IMSOb samples. Major components are indicated in bold. [a]

Fatty acids - Formulae *(name)* [a]	IMSOy	IMSOb
C16:0 *(Palmitic acid)*	3.8 ± 0.1	3.7 ± 0.1
C18:0 *(Stearic acid)*	2.6 ± 0.1	2.4 ± 0.1
C18:1c9 *(Oleic acid)* + C18:1c11 *(cis-Vaccenic acid)*	**38.8 ± 0.3**	**39.0 ± 0.2**
C18:2c9c12 *(Linoleic acid)*	**28.9 ± 0.2**	**28.9 ± 0.2**
C18:3c9c12c15 *(Linolenic acid)*	**15.1 ± 0.1**	**15.3 ± 0.1**
C20:1c9 *(Gadoleic acid)*	4.7 ± 0.1	4.7 ± 0.1
C22:1c13 (*Erucic acid*)	6.1 ± 0.1	6.0 ± 0.1
Total	100.0	100.0
Saturated species	6.5 ± 0.2	6.1 ± 0.1
Monounsaturated species	49.5 ± 0.2	49.8 ± 0.1
Polyunsaturated species	44.0 ± 0.1	44.1 ± 0.1
$\overline{M_w}$ as FFAs	284.6 ± 0.1	284.6 ± 0.0
$\overline{M_w}$ as FAEEs (2E1H esters)	312.6 (396.8)	312.6 (396.8)

[a] Fatty acid profiles were determined by methanolysis according to the ASTM-D1983 standard (**ASTM D1983-90, 1995**) for a complete conversion of the IMSO glycerides into FAMEs which were further quantified by gas chromatography (**Table A1**, Appendix A) (**EN-14103, 2011; Nitièma-Yefanova et al., 2016**); the standard deviations report the cumulative errors made during methanolysis and quantification. [b] For example, C18:1c9 means an 18 carbon fatty acid chain with one *cis* double bond (c) located at carbon 9 (starting from the carboxylic group).

Table 2. Key properties of the IMSOy and IMSOb samples used as feedstocks for ethanolysis.

Key properties	IMSOy	IMSOb
Average molecular weight [a]	891.7 ± 0.4	891.9 ± 0.1
Water content (wt %) [b]	0.044 ± 0.002	0.045 ± 0.002
Acid value (mg KOH/g) [c]	0.91 ± 0.01	0.90 ± 0.01
Acidity (%) [c]	0.46 ± 0.01	0.45 ± 0.01
Sulfur content (mg/kg) [d]	21.42 ± 0.04	8.03 ± 0.04
Tin content (mg/kg) [d]	32.01 ± 0.02	36.28 ± 0.02

[a] Calculated from the oil molar composition in terms of fatty acids. [b] Determined by Karl-Fischer titration method (**EN-ISO-12937, 2000**). [c] Determined by following the standard EN-14104 (**EN-14104, 2003**). [d] Determined by ICP-AES (**Table A1**, Appendix A) (**Pohl et al., 2010; Caumette et al., 2010; Nitièma-Yefanova et al., 2015**).

951 **Table 3.** Operating conditions of the most relevant experiments and corresponding ester contents obtained. Each operation variable (temperature,
952 ethanol to oil molar ratio, catalyst mass concentration, mass fraction of glycerol added) were changed sequentially (when changing one variable,
953 the others were remained constant). Optimal operating conditions are indicated in bold. [a]

Experiment	T/°C	Ethanol to oil molar ratio	[KOH] (wt %) [b]	Mass fraction of glycerol (wt %) [c]	Ester content (wt %) 1rst stage (30 min)	Ester content (wt %) 2nd stage (50 min)	Ethanolysis & Separation Yield (wt %)
				IMSOy (Yellow seeds)			
1	35	6: 1	1.1	25	77	83	88
2	35	8: 1	1.1	25	82	87	95
3	25	8 : 1	1.1	25	80	85	96
4	78 (1rst stage) / 35 (2nd stage)	8 : 1	1.1	25	79	87	89
5	78 (1rst stage) / 25 (2nd stage)	6 : 1	1.1	25	63	72	82
6	35	10 : 1	1.1	25	83	88	95
7	35	12 : 1	1.1	25	82	87	97
8	35	8 : 1	1.1	25 / Recycled glycerol (from Exp. 2)	80	87	94
9	35	6: 1	1.1	35 / Recycled glycerol (from Exp. 1)	79	82	88

954

955 **Table 3.** Continued. [a]

Experiment	T/°C	Ethanol to oil molar ratio	[KOH] (wt %) [b]	Mass fraction of glycerol (wt %) [c]	Ester content (wt %) 1rst stage (30 min)	Ester content (wt %) 2nd stage (50 min)	Ethanolysis & Separation Yield (wt %)
				IMSOb (Brown seeds)			
10	35	6: 1	1.1	25 / Recycled glycerol (from Exp. 1)	78	84	90
11	**35**	**8:1**	**1.1**	**25 / Recycled glycerol (from Exp. 2)**	**82**	**87**	**95**
12	35	8:1	1.6	25 / Recycled glycerol (from Exp. 2)	85	88	87
13 [d]	**35**	**8:1**	**1.1**	**25 / Recycled glycerol (from Exp. 4)**	**82**	**88**	**100**

956 [a] Stirring speed set to 250 rpm during the first stage and the first 5 min of the second stage. [b] 1.1 wt % = 1.0 + x wt %, with *x* calculated given the
957 IMSO acid value. [c] On basis of the initial oil mass; addition always conducted at 35°C, except for exp. 5 for which temperature was reduced to
958 25°C; [d] Larger scale test (×3).
959

960 **Table 4.** Characterization of produced IMSOEEs with regards to their organic and inorganic components before and after dry-purification [a].
961 Efficiency of the dry-purification method for the focused contaminants is also given in brackets. [b]

Treatment stage of the FAEE product	Esters (wt %)	Free glycerin (wt %)	MGs (wt %)	DGs (wt %)	TGs (wt %)	Total glycerin (wt %)	Water (mg/kg)
Unpurified IMSOEEs of departure	88.5	0.06	2.58	0.75	0.27	0.86	343
IMSOEEs after dry-purification	95.8 (+8)	0.01 *(-83)*	2.46 *(-5)*	0.53 *(-29)*	0.22 *(-19)*	0.72 *(-16)*	647 *(+87)*
Specifications of EN-14214 [c]	**96.5**	**0.02**	**0.80**	**0.20**	**0.20**	**0.25**	**500**

962

	Chemical element contents (mg/kg) [d]							
	Ca	Fe	K	Mg	Na	P	S	Sn
Unpurified IMSOEEs of departure	< 0.001	< 0.003	104.9	< 0.001	< 0.073	< 0.006	< 0.038	28.00
IMSOEEs after dry-purification	< 0.001	< 0.003	< 0.031 *(-100)*	< 0.001	< 0.073	< 0.006	< 0.038	25.53 *(-9)*
Specifications of EN-14214 [c]	**5** [e]	**-** [f]	**5** [g]	**5** [e]	**5** [g]	**10**	**10**	**-** [f]

963

	Percent mass composition of the identified FAEEs							
	C16:0	C18:0	C18:1 (oleate)	C18:1 (cis-vaccenate)	C18:2	C18:3	C20:1	C22:1
Unpurified IMSOEEs of departure	3.16	2.01	31.87	2.41	25.47	13.73	4.13	572
IMSOEEs after dry-purification	3.41	2.14	33.82	2.56	27.03	14.57	6.02	6.26

964 [a] Standard deviations (wt %): 0.08 on esters, 0.003 on free glycerin, 0.05 on MGs, DGs, and TGs. [b] Method efficiency assessed as a function of removal
965 percentage of each contaminant (η_c) calculated by $\eta_c = 100\times(x_f - x_0)/x_0$, where x_0 and x_f are the contents of each contaminant before and after treatment. [c] All
966 indications are limits, except for the ester content giving the maximum value. [d] Detection limits (mg/kg) of the analytical method used (ICP-AES): 0.001 for Ca

967 and Mg; 0.003 for Fe; 0.031 for K; 0.073 for Na; 0.006 for P; 0.038 for S; 0.023 for Sn; Maximum standard deviation (mg/kg): 0.001 for Ca, Mg, Fe, P, and Sn;
968 0.05 for Na; 0.01 for K and S; regarding contaminant content below or equal to the observed ICP-AES detection limit, this latter value was used to evaluate the
969 treatment efficiency. It should be mentioned that some other metals have not been detected (Ag, Al, As, B, Ba, Cd, Co, Cr, Cu, Hg, Li, Mn, Mo, Ni, Pb, Sb, Sr,
970 Ti, V, and Zn). [e] For (Ca + Mg). [f] No specification exists regarding this species. [g] For (Na + K).
971

Table 5. Operating conditions of ethyl biodiesel (IMSOEEs) conversion along with key results of biolubricant (IMSO2E1HEs) synthesis (a) and purification (b).

(a) Biolubricant synthesis

T/°C	MR (2E1H to IMSOEEs)	[KOH]/(wt %) [a]	Reaction time/min
70	2	2	65
	P/bar = 0.50	P/bar = 0.10	P/bar = 0.05
IMSOEE conversion (wt %) [b]	47.5	91.2	93.3
Biolubricant synthesis yield (wt %)	46.7	81.0	90.8
IMSOEE mass fraction (wt %)	26.4	4.4	3.4
IMSO2E1HE mass fraction (wt %)	34.8	63.8	71.2

(b) Biolubricant purification (bubble-washing & vacuum distillation) [c]

Treatment stage of the IMSO2E1HE product	K (mg/kg)	IMSOEEs (wt %)	IMSO2E1HEs (wt %)	2E1H (wt %)	Ethanol (wt %)
Unpurified IMSO2E1HEs of departure	7600 [d]	4.42	63.79	27.26	0.01
IMSO2E1HEs after purification	0.29	5.44	88.17	Not detected	Not detected

	Percent mass composition of the identified IMSO2E1HEs (IMSOEEs)							
	C16:0	C18:0	C18:1 (oleate)	C18:1 (cis-vaccenate)	C18:2	C18:3	C20:1	C22:1
Unpurified IMSO2E1HEs of departure	2.36 (0.15)	1.48 (0.10)	22.76 (1.60)	1.76 (0.13)	18.21 (1.29)	9.64 (0.67)	3.87 (0.20)	3.70 (0.26)
IMSO2E1HEs after purification	3.35 (0.19)	2.11 (0.19)	32.17 (2.01)	2.49 (0.15)	24.77 (1.67)	12.57 (0.79)	5.63 (0.27)	5.25 (0.34)

[a] On basis of the initial IMSOEE mass; the residual catalyst content (from IMSO conversion into IMSOEEs by KOH catalyzed ethanolysis) was not counted. [b] IMSOEE conversion (wt %) = $(\bar{x}^0_{IMSOEEs} - \bar{x}^t_{IMSOEEs})/\bar{x}^0_{IMSOEEs} \times 100$ where $\bar{x}^0_{IMSOEEs}$ and $\bar{x}^t_{IMSOEEs}$ are mass fractions in IMSOEEs at respectively time 0 and time t of the reaction. [c] Sample purified: IMSO2E1HEs obtained at P/bar = 0.10. See **Table A1** (Appendix A) for details regarding the analysis methods selected. For K quantification by ICP-AES, detection limit and maximum standard deviation: 0.031 and 0.01 mg/kg, respectively. Like esters, the two alcohols were quantified by GC-FID (**Table A1**, Appendix A). [d] Value estimated on the basis of the amount of catalyst used for the biolubricant synthesis.

Table 6. Some specific functional properties of the produced biofuel (IMSOEEs) and biolubricant (IMSO2E1HEs) – Comparison with corresponding standard quality specifications. [a]

Property	IMSOEEs biofuel	Biodiesel specifications		IMSO2E1HEs biolubricant	RO2E1HEs biolubricant (Ineos, 2018)	Standard deviations [b]
		min	max			
Acid value (mg KOH/g)	0.34	-	0.50	12.2	0.5	± 0.02
Color (Gardner)	10.4	-	-	4.7	1.0	± 0.2
Density (kg/m^3)	882 (15°C)	860 (15°C)	900 (15°C)	875 (20°C)	870 (20°C)	± 3·10^{-5}
Viscosity (mm^2/s) at 40°C	5.0	3.5	5.0	8.6	9.0	± 0.1
at 100°C		-	-	2.8	3.0	± 0.1
Flash point (°C)	425	101	-	-	200	± 12
Cloud point (°C)	-5	-12	-3	-	-	± 1
Pour point (°C)	-9	-16	-5	-	-69	± 2
Cold filter plugging point (°C)	-11	-	-	-	-	-

[a] Biofuel and biolubricant are obtained after dry-purification; see **Table A1** in Appendix A for details regarding the methods leading to the above given property values. Biolubricant properties are compared for two classes of esters obtained from the same alcohol i.e. 2E1H (2-ethyl-1-hexanol) with two different oils IMSO (Indian mustard seed oil) and RO (rapeseed oil). [b] These standard deviations are common to determination of both biofuel and biolubricant specific functional properties.

APPENDICES

Appendix A – Biodiesel & Biolubricant

Table A1. Analysis equipment and operating conditions regarding to the production, purification and characterization of biodiesel and biolubricant carried out in this work.

Objective	Experimental technique	Equipment	Operating conditions
		Biodiesel & Biolubricant production	
Monitoring of the transesterification with ethanol or 2-ethyl-1-hexanol	Off-line GC-FID with preliminary GC-MS	Agilent Technologies (USA)	•*Preliminary sample neutralization & Ester quantification:* Please refer to **Nitièma-Yefanova et al. (2016) (Appendix B, S.I.)**. •*Ester quantification*: Please refer to **Mohammad et al. (2017)** except for the oven temperature program: 60°C (2 min), 60-200°C (10°C/min), 200-240°C (5°C/min), 240°C (7 min for IMSOEEs, 16 min for IMSO2E1HEs). *After centrifugation of the sampling tubes*, 0.1 mL of the organic phase was poured in vials prefilled with 1 mL of stock solution, i.e. a mixture of well-known composition in the internal standard selected for FAEE quantification (MHD) with n-heptane. The *response factors of all FAEEs* relatively to MHD were assigned to the value obtained for ethyl oleate (major component of IMSOEEs, **Table 1**). Regarding biolubricant quantification, the *response factors of all IMSO2E1HEs* were assigned to 1 (commercial standard of 2-ethyl-1-hexyl oleate unavailable) while 1-pentanol was selected as internal standard to determine the residual 2-ethyl-1-hexanol and potential traces of ethanol. Note that MHD was used instead of methyl nonadecanoate recommended in the European standard EN-14103 of May 2011 (**EN-14103, 2011**) because of overlapping with the ethyl linoleate GC peak (**Nitièma-Yefanova et al., 2016 (Appendix B, S.I.)**).

997 **Table A1.** Continued.

Objective	Experimental technique	Equipment	Operating conditions or Standard
		Biodiesel characterization – **(a)** Dry-purification	
Glyceride (TGs, DGs, MGs), free glycerin and FAEE contents	GC-FID	INEOS Enterprises (France)	EN-14105 **(EN-14105, 2011)**, except for FAEEs: EN-14103 **(EN-14103, 2011)**
Water content	Coulometric Karl Fischer titration	INEOS Enterprises (France)	ISO-12937 **(EN-ISO-12937, 2000)**
Potassium and other elements (Ca, Fe, Mg, Na, P, S, Sn) contents	ICP-AES	ARCOS by SPECTRO; Scott-type double-pass spray chamber combined with cross-flow nebulizer (Germany)	Please, refer to **Nitièma-Yefanova et al., 2015** **(Pohl et al., 2010; Caumette et al., 2010)**
		Biodiesel characterization – **(b)** Fuel properties	
Acid value	Volumetric titration	INEOS Enterprises (France)	EN-14104 **(EN-14104, 2003)**
Color	Colorimetry	INEOS Enterprises (France)	ASTM-D1544 **(ASTM D1544-04, 2010)**
Density (15°C)	Oscillating U-tube	INEOS Enterprises (France)	ISO-12185 **(EN-ISO-12185, 1996)**
Viscosity (40°C)	Capillarity viscometer	INEOS Enterprises (France)	ISO-3104 **(EN-ISO-3104, 1996)**
Flash point	Estimation	-	Vapor-liquid equilibria estimation based on composition in FAEEs (from GC-FID), their molecular structure, and their vapor pressures as pure components **(Carareto et al., 2012)**
Cloud point	Estimation	-	Correlation based on number of carbon atoms and composition in FAEEs (from GC-FID) **(Bolonio et al., 2015)**
Cold filter plugging point (°C)	Estimation	-	Correlation based on number of carbon atoms and composition in FAEEs (from GC-FID) **(Bolonio et al., 2015)**
Pour point	Estimation	-	Correlation based on number of carbon atoms and composition in FAEEs (from GC-FID) **(Bolonio et al., 2015)**

998

Table A1. Continued.

Objective	Experimental technique	Equipment	Operating conditions
Biolubricant characterization – **(a)** Purification by bubble-washing & vacuum fractional distillation			
Monitoring of the bubble-washing	Flame-AES	Sherwood Scientific Model 410 (UK)	Air-butane flame in on emission wavelength of 769.9 nm to measure K content in washing solution; calibration with pure water and standard solutions of K.
Validation of vacuum distillation	GC-FID	Agilent Technologies (USA)	See above "Biodiesel & Biolubricant production" •Ester identification, •Ester quantification, and •HP-INNOWAX column, **Table A1**.
Biolubricant characterization – **(b)** Specific functional properties			
Acid value	Volumetric titration	INEOS Enterprises (France)	ISO-6618 **(ISO-6618, 1997)**
Color	Colorimetry	INEOS Enterprises (France)	ASTM-D1544 **(ASTM D1544-04, 2010)**
Density (20°C)	Oscillating U-tube	INEOS Enterprises (France)	ISO-12185 **(EN-ISO-12185, 1996)**
Viscosity (40 and 100°C)	Capillarity viscometer	INEOS Enterprises (France)	ISO-3104 **(EN-ISO-3104, 1996)**

Appendix B – Fine Indian mustard stems (FIMS) details as adsorbent

Details of the equipment and operating conditions selected to carry out FIMS characterization are listed in **Table B1 (Rapp et al., 2018)**.

The average particle size D [3,2] (Sauter mean diameter) measured by laser diffraction is 254 µm (the smallest particles being larger than 10 µm diameter). Morphological analysis by scanning electron microscopy (SEM) reveals a heterogeneous structure (**Figure B1**) with a heterogeneous mass composition in the main elemental components *i.e.* C, O, Ca and K, as observed when coupling SEM with microanalysis by energy dispersive X-ray spectroscopy (EDS) (**Figure B2**). Existence of macropores as noticed in **Figure B1b** is confirmed by Brunauer-Emmet-Teller (BET) method (**Figure B3**) showing a quite flat adsorption profile, specific to macroporous material of diameter larger than 50 nm, with low specific area (< 1 m^2/g) and very small pore volume (≈ 0.07 cm^3/g).

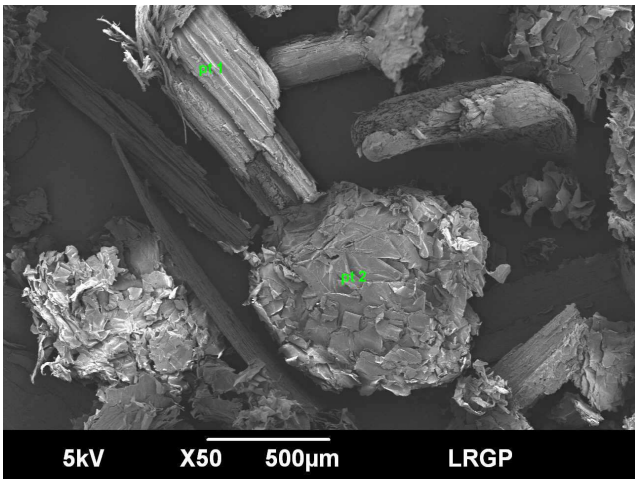

(a)

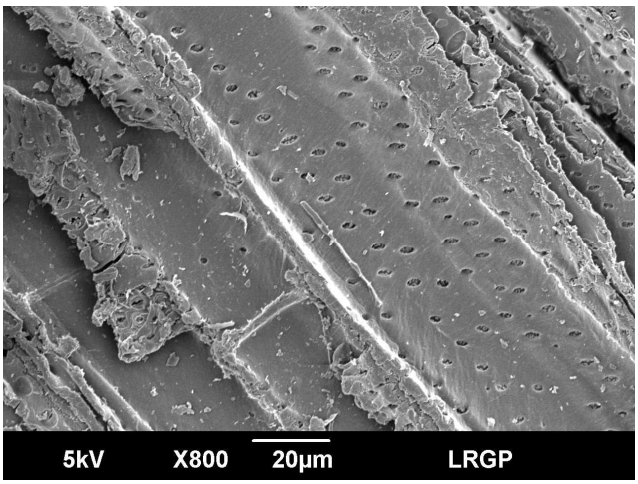

(b)

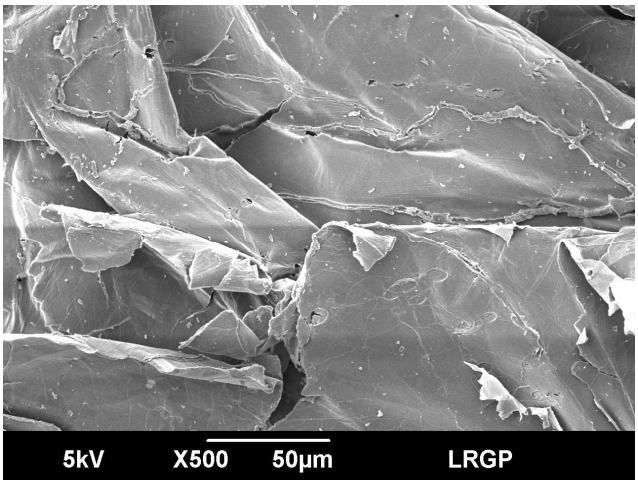

(c)

Figure B1. SEM analyses of FIMS (secondary electrons with gold-palladium coating). (a) whole sample; (b) bark (pt1); (c) core (pt2).

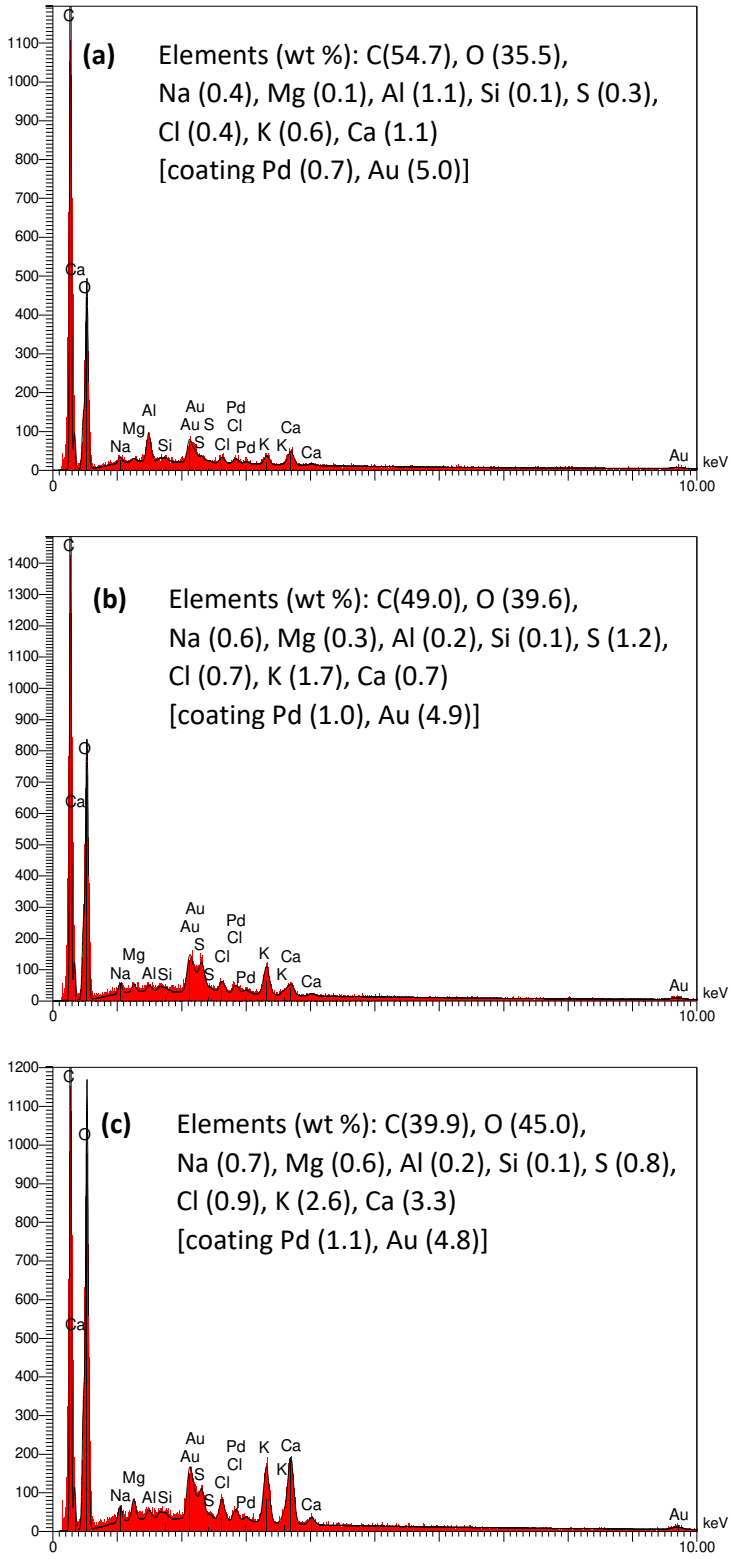

Figure B2. EDS analyses of FIMS (secondary electrons with gold-palladium coating). (a) whole sample; (b) bark; (c) core.

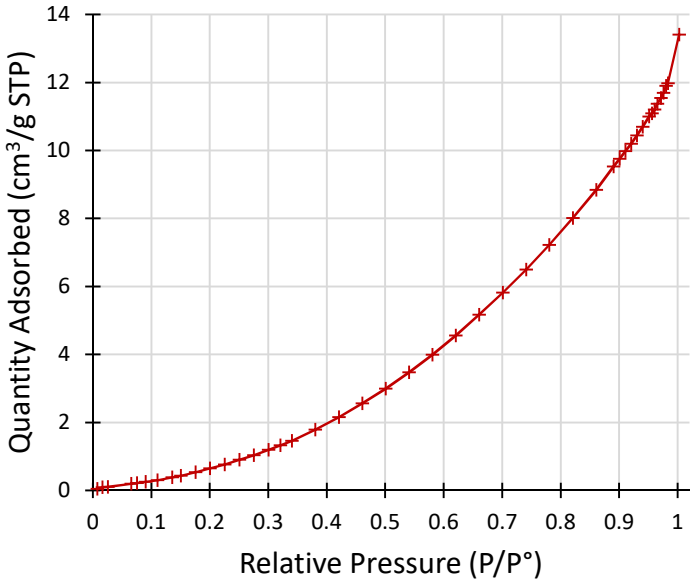

Figure B3. N_2 adsorption isotherm of FIMS.

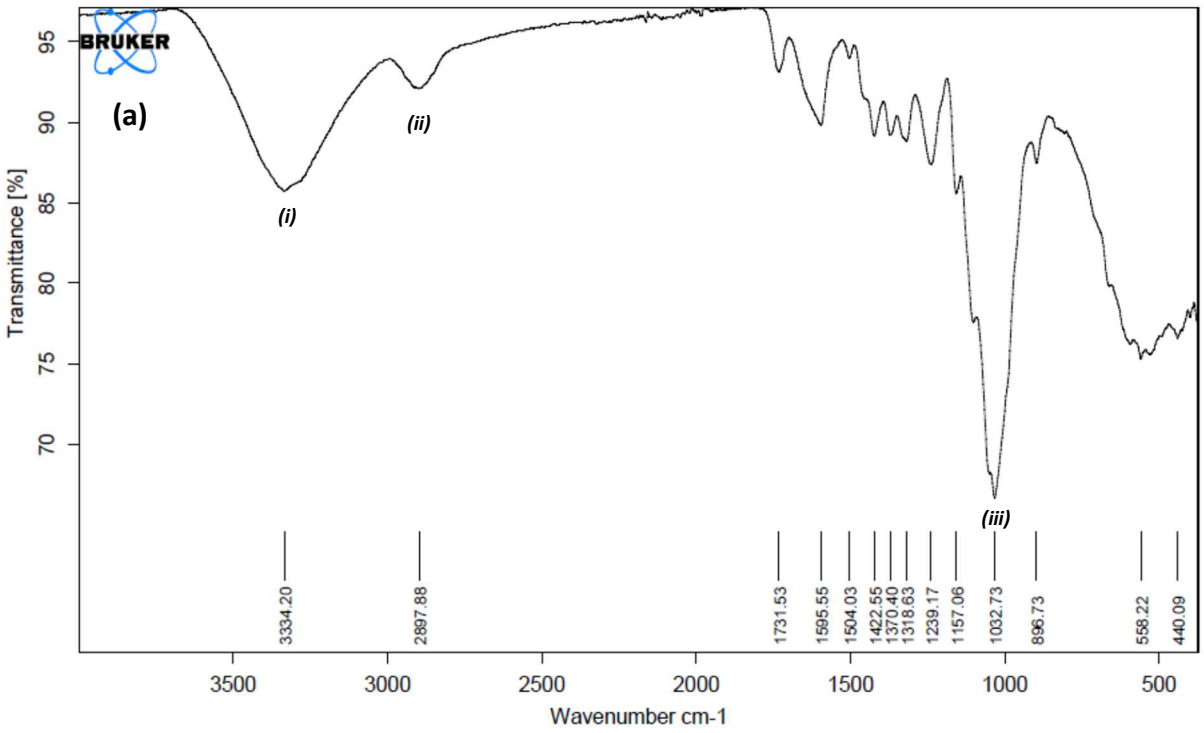

1030

1031

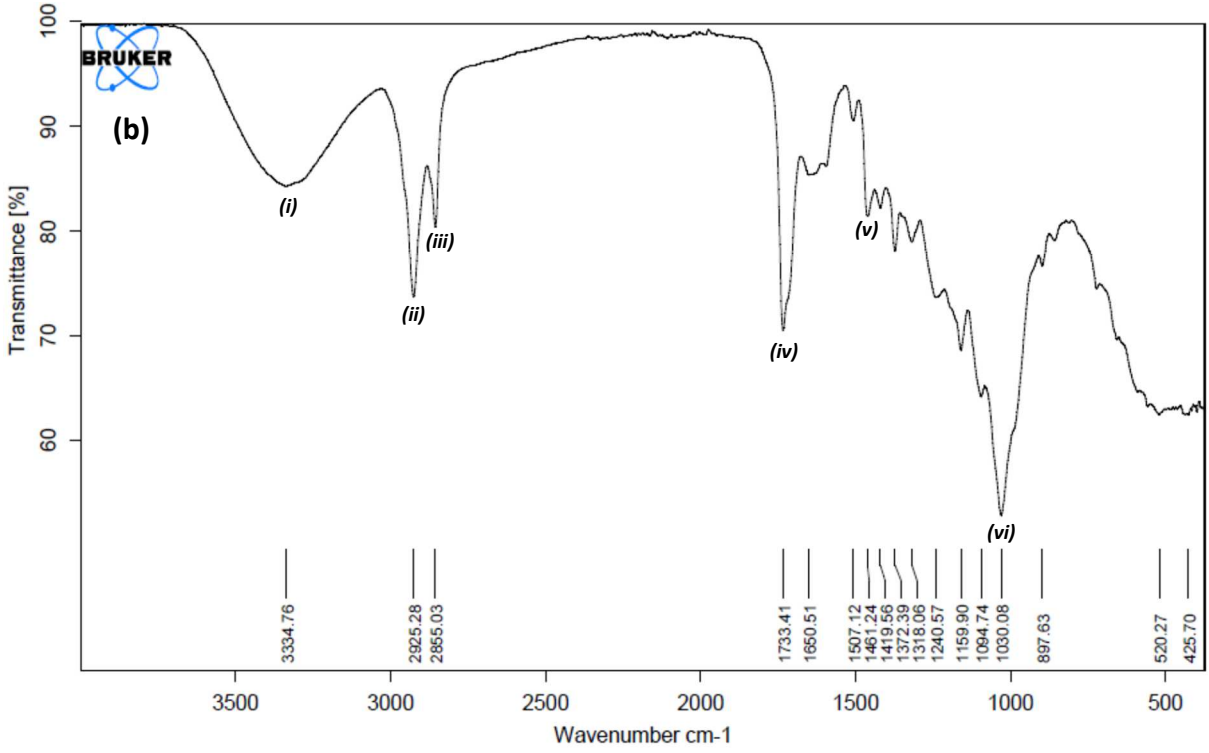

1032

1033

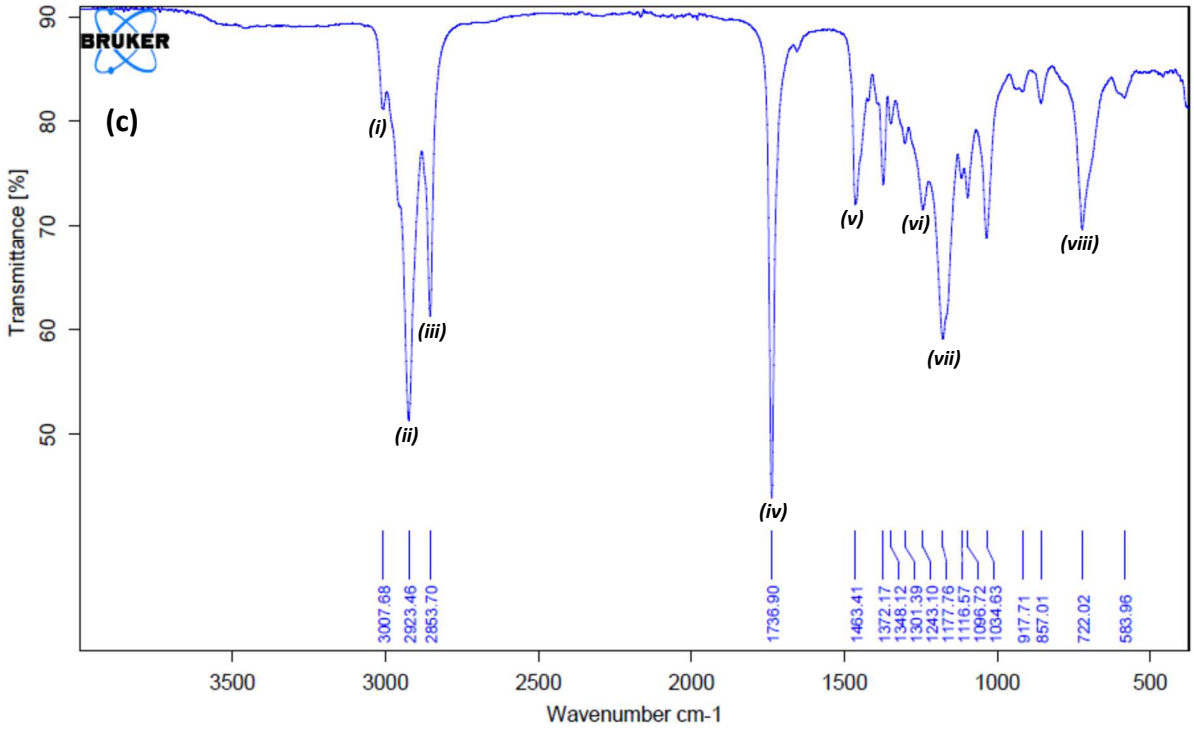

Figure B4. FTIR spectra of FIMS before **(a)** and after **(b)** use as adsorbent for biodiesel **(c)** dry-purification.

(a) *(i)* free hydroxyl O-H stretching at the range of 3500 to 3300 cm^{-1}, *(ii)* alkyl C-H stretching at 2898 cm^{-1}, *(iii)* etheric C-O stretching at 1033 cm^{-1}. **(b)** *(i)* free hydroxyl O-H stretching at the range of 3500 to 3300 cm^{-1}, *(ii)* symmetric vibration of methyl CH_3 at 2925 cm^{-1}, *(iii)* asymmetric stretching vibrations of methylene CH_2 at 2855 cm^{-1}, *(iv)* stretching of carbonyl C=O bond in an ester at 1733 cm^{-1}, *(v)* bending of CH_3 and CH_2 at 1461 cm^{-1}, *(vi)* etheric C-O stretching at 1033 cm^{-1}. **(c)** *(i)* and *(iii)* methylene symmetric and asymmetric stretching vibrations at 3008 and 2854 cm^{-1} respectively, *(ii)* prominent band attributed to symmetric vibration of CH_3 at 2923 cm^{-1}, *(iv)* intense band assigned to the stretching of C=O bond of an ester at 1737 cm^{-1}, *(v)* bending of the CH_3 and CH_2 groups at 1463 cm^{-1}, *(vi)* antisymmetric axial stretching vibrations of C-C(=O)-O bonds of the ester at 1243 cm^{-1}, *(vii)* asymmetric axial stretching vibrations of O-C-C bonds at 1178 cm^{-1}, *(viii)* out of plane deformation of the olefinic groups C=CH specific to the unsaturated derivatives in the range 900-700 cm^{-1} (**Mazivila et al., 2015; Feng et al., 2018**).

1052 **Table B1.** Analysis equipment and operating conditions selected for FIMS adsorbent characterization.

1053

Objective	Experimental technique	Equipment	Operating conditions
Average particle size (Sauter mean diameter) D[3,2]	Laser diffraction	Malvern Master sizer 2000 (UK)	Size range: 0.02 to 2000 µm
Morphology	SEM	JEOL microscope; model JSM-6490 LV (Japan)	Please, refer to **Nitièma-Yefanova et al., 2015**
Elemental chemical composition	SEM-EDS	JEOL microscope; model JSM-6490 LV (Japan) + SAMX-IDFIX system (microanalysis) (France)	Please, refer to **Nitièma-Yefanova et al., 2015**
Surface area and porosity	N_2 adsorption isotherms + BET method	Sorptomatic 1990, ThermoQuest CE Instruments (Italy)	Please, refer to **Nitièma-Yefanova et al., 2015**
Chemical structure (bonds/rings)	FTIR	Bruker Alpha-P spectrophotometer, equipped with an Attenuated Total Reflectance (ATR) crystal accessory (Switzerland)	For each spectrum: 128 scans applied at a resolution of 4 cm^{-1} with the wavenumber ranging from 4000 to 375 cm^{-1}

1054